issn 0065-3713

INSTITUT D'AERONOMIE SPATIALE DE BELGIQUE

3 - Avenue Circulaire
B - 1180 BRUXELLES

AERONOMICA ACTA

A - N° 330 - 1988

General equations for the motions of ice crystals and water drops in gravitational and electric fields

by

JOHN S. NISBET

BELGISCH INSTITUUT VOOR RUIMTE-AERONOMIE

3 - Ringlaan
B - 1180 BRUSSEL

FOREWORD

The paper entitled "General Equations for the Motions of Ice Crystals and Water Drops in Gravitational and Electric Fields" has been submitted for publication in Annales Geophysicae.

AVANT-PROPOS

L'article intitulé "General Equations for the Motions of Ice Crystals and Water Drops in Gravitational and Electric Fields" a été soumis pour publication dans Annales Geophysicae.

VOORWOORD

Het artikel "General Equations for the Motions of Ice Crystals and Water Drops in Gravitational and Electric Fields" werd voorgelegd ter publikatie in Annales Geophysicae.

VORWORT

Der Artikel "General Equations for the Motions of Ice Crystals and Water Drops in Gravitational and Electric Fields" wurde vorgestellt zur Publikation in Annales Geophysicae.

GENERAL EQUATIONS FOR THE MOTIONS OF ICE CRYSTALS AND WATER DROPS IN GRAVITATIONAL AND ELECTRIC FIELDS

by

John S. Nisbet

Communications and Space Sciences Laboratory, Penn State University, 316 EEE, University Park, Pa 16802, USA. Presently at the Institut d'Aéronomie Spatiale de Belgique, Ave Circulaire 3, 1180 Bruxelles, Belgique, and l'Université Paul Sabatier, Toulouse, France.

ABSTRACT

The technique of fitting with asymptotic functions has been used to develop simple equations relating the forces for a variety of types of ice crystals and water drops and droplets in terms of the Davies, Bond and Knudsen numbers to the Reynolds numbers and hence to the velocities. Equations are also given, in a common format suitable for incorporation in computer models, of the sedimentation velocity and mobility as functions of the atmospheric pressure level and an appropriate length parameter for each particle type.

RÉSUMÉ

La technique d'ajustement à l'aide de fonctions asymptotiques a été utilisée pour déduire des équations simples reliant les forces au nombre de Reynolds donc aux vitesses pour plusieurs types de cristaux de glace, des gouttes et des gouttelettes d'eau en termes des nombres de Davies, Bond, et Knudsen. Des équations de la vitesse de sédimentation et de la mobilité en fonction de la pression atmosphérique et d'une dimension caractéristique pour chaque type de particule sont également données dans un format utile pour l'incorporation dans des codes numériques.

SAMENVATTING

De aanpassingstechniek met behulp van asymptotische functies werd gebruikt om eenvoudige vergelijkingen af te leiden die een verband leggen tussen de krachten voor een aantal types ijskristallen, waterdruppels en druppeltjes in termen van de Davies, Bond, en Knudsen getallen tot de Reynolds getallen en daarom tot de snelheden. Vergelijkingen werden eveneens gegeven, in een algemeen formaat geschikt om opgenomen te worden in computer modellen, van de sedimentatiesnelheid en beweeglijkheid in functie van de atmosferische druk en een geschikte lengte-parameter voor elk soort deeltje.

ZUSAMMENFASSUNG

Die Anpassungstechnik mit der Hilfe von asymptotischer Funktionen wurde benutzt um Vergleichunggen ab zu leiten, die einen Zussammenhang machen zwischen den Kräften für mehrere Typen Eiskristallen, Wassertropfen und Wassertröpfchen nach dem Wortlaut der Davies, Bond und Knudsen Zahlen, und der Reynolds Zahlen, und folglich der Geschwindigkeiten. Vergleichungen sind auch gegeben, in einem geeigneten Format für nümerische Modellen, der Absetsgeschwindigkeit und der Beweglichkeit wie Funktionen des atmosphärischen Druckes und ein geeignete Längenparameter für jede Partikel.

1. INTRODUCTION

The motions of hydrometeors in the gravity and electric fields of a thundercloud are of prime importance in understanding the generation, neutralization, accretion and transport processes. At the upper end of the mass spectrum are the hail and graupel particles with sizes of the order mm to cm, while at the lower end cloud conductivities are controlled by cloud droplets as small as a few microns in diameter. Because gravitational forces are proportional to the volume while the electrical forces may be more closely proportional to the surface area the size spectrum of interest when electrification is involved generally extends below that which must be considered when all the particles are neutral.

For several processes it is the differences in velocities between different types and sizes of particles that are critical. Currents are produced when relative motion occurs between charged particles of opposite polarities. It is upon the differences in velocities that the collision rates depend which control charge transfer and accretion for example. Electrical forces are particularly important in controlling collisions between charged particles. Charge build up occurs wherever there is a divergence in the current density and so factors such as the altitude gradient of the velocities are important.

The implications of transport to, for example, mass fluxes, current densities, or collision rates depend on integrals over the range of types and sizes of particles present and so it is necessary to have statistical parameters that can be used for such calculations.

The number of different types and sizes of particles that needs to be considered in a cloud electrification model can be large and so it becomes important to have reasonably efficient subroutines for the calculation of the transport properties. In particular it is advisable not to have to check, the force for example, before choosing an appropriate formula for a calculation. The development of such equations is the aim of the present study.

2. GENERAL RELATIONS

The momentum continuity equation may be written,

$$F = - m (dU/dt + g) + q E = - D \qquad (1)$$

where,

	D	is the drag force,	(N)
	m	is the mass of the particle,	(kg)
	U	is the particle velocity,	(m s^{-1})
	t	is the time,	(s)
	g	is the gravitational acceleration	(m s^{-2})
	q	is the charge on the particle,	(C)
and	E	is the electric field.	(V/m)

The drag force on solid particles is a function of the relative velocity and the density and viscosity of the surrounding air.

It is convenient to work in dimensionless parameters. The parameter, which is conventionally used, related to the force is the Davies or Best number, Davies [1945], Best [1950],

$$N_D = (8 \rho / \pi \eta^2) F \qquad (2)$$

where	η	is the dynamic viscosity of air	(kg/m s)
	ρ	is the air density	(kg m^{-3})

The Reynolds number is,

$$N_R = (\rho d / \eta) (U - U_a) \qquad (3)$$

where	U	is the particle velocity	(m/s)
	U_a	is the air velocity	(m/s)
and	d	is the particle diameter	(m)

The mean free path at cloud altitudes is of the order of 10^{-7} m and for cloud particles smaller than about 10^{-5} m the drag force becomes a function of the ratio of the mean free path to the particle diameter, the Knudsen number.

$$N_K = l / d \qquad (4)$$

where l is the mean free path

The force on a particle can be calculated from the electric field strength and particle mass and charge. The calculation of the velocities of solid particles thus involves determining the functional relation of the Davies and Knudsen numbers to the Reynolds number.

2.1. SPHERICAL PARTICLES

Let us first examine the drag forces on spherical particles. The Reynolds number is related to the Davies number by the relation,

$$N_R = [N_D / C_d]^{1/2} \qquad (5)$$

where C_d is the drag coefficient.

Terminal fall velocities for large graupel and hail have been given by Bilham and Relf [1937], List [1959], Macklin and Ludlam [1961], Auer [1972a] and Roos [1972]. In the range of Reynolds numbers between 1000 and 5000, corresponding to particles in the size range from about 1 to 5 mm depending on the altitude and particle density, the drag coefficient C_d is not greatly dependent on Reynolds number and the relative velocity of the particle is given by,

$$U - U_a = [8 F / (\pi \rho C_d)]^{1/2} / d \quad (m/s) \qquad (6)$$

For the range of Reynolds numbers between 10^{-6} and 10^{-2} corresponding to particle diameters in the range from 10^{-6} m to $2\ 10^{-5}$ the flow is laminar and the Knudsen number lies between 0.003 and 0.015 over the range of densities normally encountered in clouds. Drag forces on spherical particles in this regime have been treated by Knudsen and Weber [1911], Epstein [1924], Davies [1945], Beard [1976], and others.

The drag force in this region is given by first-order correction to the Stokes equation,

$$N_R = N_D (1 + 2.5 N_K) / 24 \quad (7)$$

In this range of Reynolds numbers the relative velocity of the particle is given by,

$$U - U_a = F (1 + 2.5 l/d) / (3 \pi \eta d) \text{ (m/s)} \quad (8)$$

The range of Reynolds numbers between these two regimes is of considerable importance because it corresponds to diameters between 2 10^{-5} m and 10^{-3} m and includes the major part of the precipitation particles in the cloud. It is in this region however, that the flow changes from laminar to turbulent and the relation between the drag force and the velocity changes markedly. At Reynolds numbers below 10 the relative velocity is proportional to the Davies number and at Reynolds numbers above 1000 proportional to the square root of the Davies number. It is thus apparent that the drag coefficient and its altitude variation are both functions of the Reynolds number in this region. Theory as well as sea level measurements are thus necessary to obtain altitude dependant drag coefficients.

LeClair et al. [1970] have presented equations for the drag coefficient in terms of the Reynolds number for $0.01 < N_R < 20$, Beard and Pruppacher [1969] for $20 < N_R < 258$, and Perry [1950] for $258 < N_R < 5000$. Such equations are difficult to use when it is desired to calculate the velocity from the force.

It has been common following Davies [1945] to make empirical polynomial fits to the relationship of the logarithm of the Davies number to the logarithm of the Reynolds number. This technique has been used, for example, by Heymsfield [1972] for a variety of types of ice crystals and by Beard [1976] for cloud and precipitation drops. The method provides good fits to the sedimentation velocities providing the range of Reynolds numbers is not too large, however, the coefficients in the equations for adjacent ranges differ considerably and the fits using higher order polynomials deteriorate very rapidly outside their range. These problems are aggravated when electric forces are considered because the Reynolds number is no longer a unique function of the particle diameter so that checks have to be put into computer programs to ensure that the correct formula is used. The fluctuations in the first derivative of the relationship between the Reynolds number and the Davies number appear

to be of the order of 15% over the range from 10 to 1000 in Reynolds number due to the form of the function used for the fit alone. The calculated mobilities depend on these derivitaves. Moreover, though the formulas are continuous for the Reynolds number at the boundaries, they are not for the first derivative, and so discontinuities are introduced in the mobilities between ranges.

Abraham [1970] presented a model of a blunt body passing through a viscous medium based on boundary layer theory which results in a relation between the drag coefficient and the Reynolds number that agrees well with experiment over a wide range of Reynolds numbers.

$$C_d = C_A \left(N_o^{-0.5} + N_R^{-0.5} \right)^2 \qquad (9)$$

C_d from equation (9) when used in equation (5) provides an asymptotic fit to the function in equation (7) after applying the Knudsen number correction term. It also provides good agreement with relations given by LeClair et al. [1970], Beard and Pruppacher [1969],and Perry [1950]. It is apparent that, despite the complexities of the transitions that occur in the flow patterns over this very extensive range of Reynolds numbers, the Abraham relation provides good agreement with empirical relationships expressed in polynomial expressions each applicable to a much more limited range. The Abraham [1970] relation is not convenient to use to calculate velocities from forces because it expresses the Davies number in terms of the Reynolds number and not vice versa. It did indicate, however, that the technique of using asymptotic matching functions might provide a simple relation of the Reynolds number to the Davies number in which the coefficients were related to physical parameters.

It is apparent that a function of the form,

$$N_R = \left(1 + 2.5\, N_K \right) / \left(A\, N_D^{-1} + F_m + C\, N_D^{-0.5} \right) \qquad (10)$$

would provide an asymptotic fit to equations (5) and (7) as N_D tends to zero and infinity provided the matching function F_m is chosen appropriately. A suitable form for F_m is given by a series of terms of the form

$$F_m = \Sigma (a_i N_D^{ni}) \quad -1 < n_i < -0.5 \qquad (11)$$

For most atmospheric modeling purposes a single term with n = -0.75 appears to give an adequate fit.

By fitting to the relations given by LeClair et al. [1970] for $0.01 < N_R < 20$, Beard and Pruppacher [1969] for $20 < N_R < 258$, and by Perry [1950] for $258 < N_R < 5000$ the following expression was obtained,

$$N_R = (1+2.5\ N_K)/(b_1\ N_D^{-1}+b_2\ N_D^{-0.75}+b_3\ N_D^{-0.5}) \qquad (12)$$

where,

$b_1 = 21.786$
$b_2 = 2.3836$
$b_3 = 0.5590$

From equation (2),

$$N_D = 8\ \rho\ /\ \eta^2\ [\ (g\ \Delta\rho\ /\ 6\ )\ d^3 + E\ C_q\ d^2\ ] \qquad (13)$$

where $\Delta\rho$ (kg/m^3) is the difference between the particle and air density
and C_q (C/m^2) is the charge per unit area on the particle

From equation (3),

$$U - U_a = (\ \eta\ /\ \rho\ d\ )\ N_R \qquad (14)$$

Using the effective collision diameter of mean air from the US Standard Atmosphere [1976] in equation (4) gives,

$$N_K = 2.33E\text{-}10\ T\ /\ (\ p\ d\ ) \qquad (15)$$

where T is the air temperature (K)
and p is the atmospheric pressure (bar)

Equations (12) to (15) above may be combined for the case of no electric field to give the terminal fall velocity to be,

$$U-U_a = (1+2.5N_K)/\ \Sigma_3(\ a_i\ \Delta\rho^{ci}\ d^{di}\ \rho^{ei}\ \eta^{fi}\ )\ (m/s) \quad (16)$$

The values for the coefficients in this expression are given in Table 1

TABLE 1

i	a_i	c_i	d_i	e_i	f_i
1	1.6656	-1.0	-2	0	1.0
2	0.3466	-0.75	-1.25	0.25	0.5
3	0.1546	-0.5	-0.5	0.5	0.0

Figure 1 shows a comparison between the sedimentation velocities in the absence of an electric field calculated using equation (16) with those given by the relation of Beard [1976] for the range of diameters between 0.5 microns and 20 microns. Figure 2 is a similar comparison with the relations given by LeClair et al. [1970], Beard and Pruppacher [1969], and Perry [1950] from 20 microns to 6 mm.

2.2 PLANE FORM CRYSTALS

Jayaweera and Cottis [1969] studied the relationship between the force and the drag on circular and hexagonal plates over a range of Davies numbers from about 1 to 10^4. They concluded that for plate-like forms the relationship between the Reynolds number and the Davies number is almost independent of the ratio of the thickness t to the width W. As was done with the spherical forms the data of Jayaweera and Cottis [1969] were fitted by the expression,

$$N_R = (1 + 2.5\ N_K)/(b_1\ N_D^{-1}+b_2\ N_D^{-0.75}+b_3\ N_D^{-0.5}) \quad (17)$$

which gave $b_1 = 11.71$

$b_2 = 3.654$

$b_3 = 0.6586$

where $N_D = (\ 8\ \rho\ /\ \pi\ \eta^2\ )\ F$ (18)

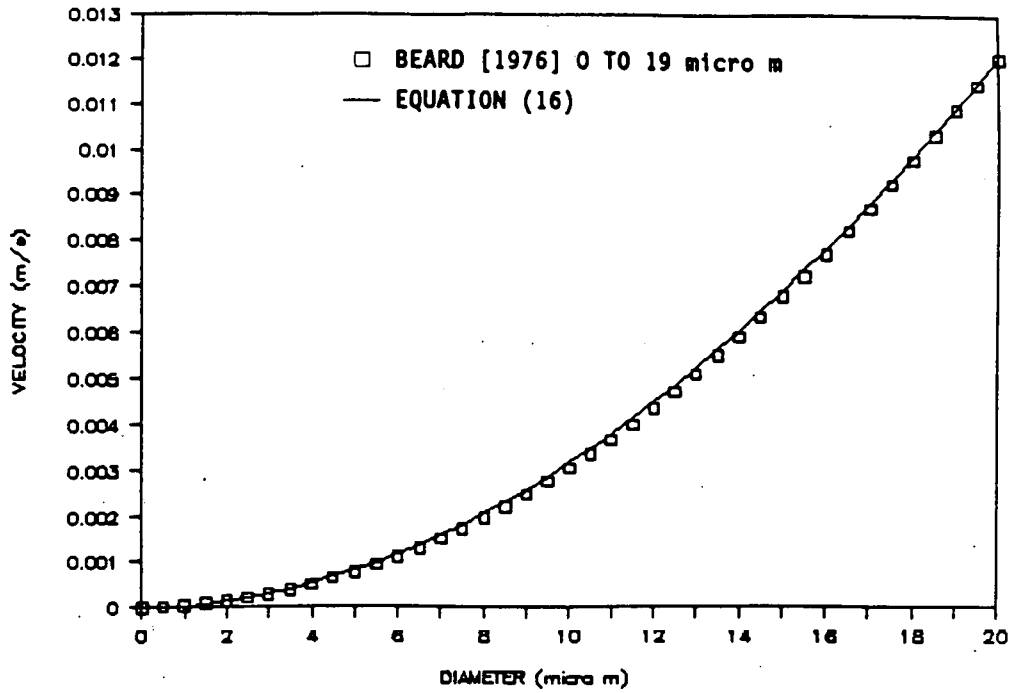

Figure 1. Comparison of the sedimentation velocity in the absence of an electric field for spherical particles given by Equation (16) with those given by the Beard (1) relation, p = 1000 mb, $\Delta\rho$ = 1000 kg/m^3.

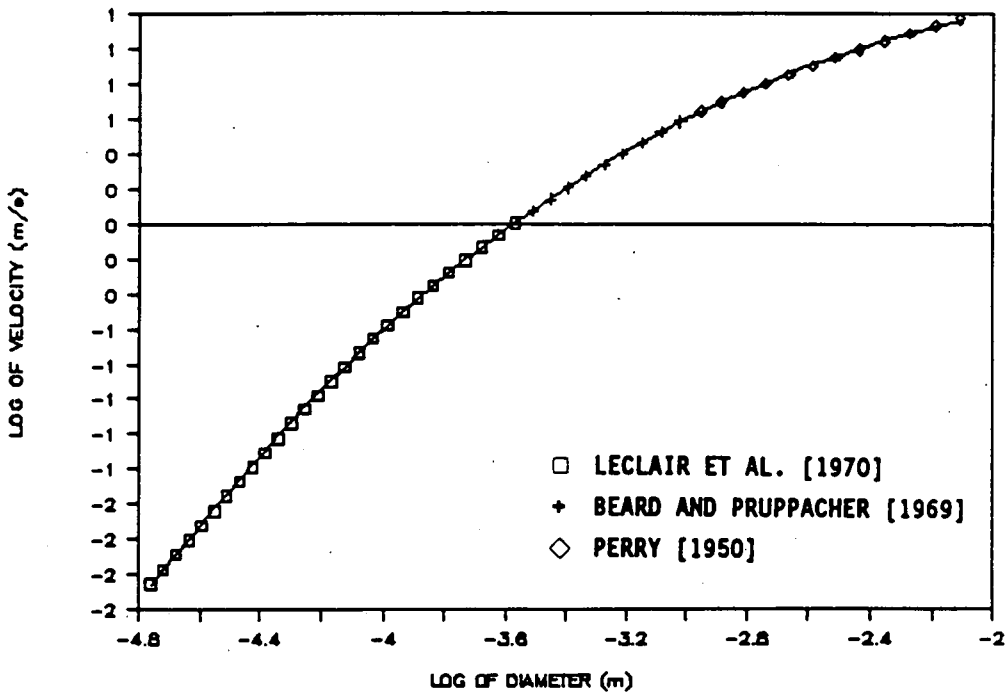

Figure 2. Comparison of the sedimentation velocity in the absence of an electric field for spherical particles given by Equation (16) with those given by LeClair et al. [1970], Beard and Pruppacher [1969], and Perry [1950], p = 1000 mb, $\Delta\rho$ = 1000 kg/m^3.

Kajikawa [1971] and List and Schemenauer [1971] and Jayaweera [1972] have given relations between the Davies and Reynolds numbers for different shapes of plate-like ice crystals. List and Schemenauer [1971] have given an equation for the drag coefficient C_d as a function of the area of the crystal A_C to the area of a circular disc A_D of the same width that allows equation (17) to be used for all crystals of plane form.
This gives,

$$U - U_a = 1.34\, N_R\, \eta/(\rho\, W\, (1+ 0.96\, A_C/A_D)^{0.5}) \quad (m/s) \quad (19)$$

$$A_s = (\, A_C/A_D\,)\, \pi\, W^2 / 2 \quad (m^2) \quad (20)$$

$$F = m\, g + A_s\, C_q\, E \quad (N) \quad (21)$$

Table 2 gives values for the ratio of the area of various plane form crystals to the area of a circular disk and of the ratio of the velocities for the same force F and width W from the data of List and Schemenauer [1971].

TABLE 2

CRYSTAL TYPE	A_C/A_D	U_C-U_a/U_D-U_a
Thick Plates	0.834	1.04
Hexagonal Plates	0.834	1.04
Sectorlike Branches	0.736	1.07
Broad Branches	0.473	1.18
Stellar Forms	0.277	1.24
Dendrites	0.182	1.29

Heymsfield [1972], Kajikawa [1972], Hobbs et al. [1974], and Locatelli and Hobbs [1974] have made measurements of the dimensions and masses for various types of plane crystals that can be used to calculate general relations for transport velocities.

Magono and Lee [1966] have suggested a subjective classification of snow crystals into eighty classes which has been widely adopted. It is, however, useful to have a numerical coordinate system in which the statistical properties appropriate to transport of a group of crystals can be specified. It is desirable

to have a single parameter which characterizes the crystal size and another which corresponds as far as possible to a given type of crystal. Figure 3 shows measurements of the equivalent diameters of the drops formed on melting plane form crystals measured by Kajikawa [1972]. Superimposed on these data are lines given by the equations,

$$m = m_0 \left(W / d_0 \right)^N \quad \text{(kg)} \quad (22)$$

where $$m_0 = \left(\pi \Delta\rho_0 / 6 \right) d_0^3 \quad \text{(kg)} \quad (23)$$

This expression tends to the mass of a sphere of density $\Delta\rho_0$ as the diameter tends to d_0. The values used for d_0 and $\Delta\rho_0$ are not very critical as far as fitting the data in Figure 3 is concerned, however, they do affect the values of N. A value of 10^{-5} m for d_0 and of 1000 (kg/m^3) for $\Delta\rho_0$ have been adopted here because they appear to organize the data reasonably well for the thinner and lighter crystals. Kumai [1961] found the sizes of microspherule central nuclei of ice crystals varied from $5\ 10^{-7}$ to $8\ 10^{-6}$ m. Auer [1971] found the average size of frozen cloud droplet embryos of planar ice crystals to be $1.1\ 10^{-5}$ m and Auer [1972b] reported values near $2.5\ 10^{-5}$ m. The value adopted appears to be reasonably consistent with both these modes of nucleation. Heymsfield [1972] presented data showing that measurements of the density of a variety of plane form crystals tended to 1000 (kg/m^3) as their diameters decreased.

Table 3 gives values of N calculated from data given by a number of investigators. It may be seen from an examination of the data in Figure 3 that there is a large spread in the mass of crystals of each form for any given width. If ice physics were constraining crystal growth into a series of discretely different forms then a distribution of probability as a function of N with a strong central maximum would be expected for each type. Instead the distributions appear to be quite uniform in each category suggesting a more or less continuous range of crystal habits with the selection criteria controlling the limiting values.

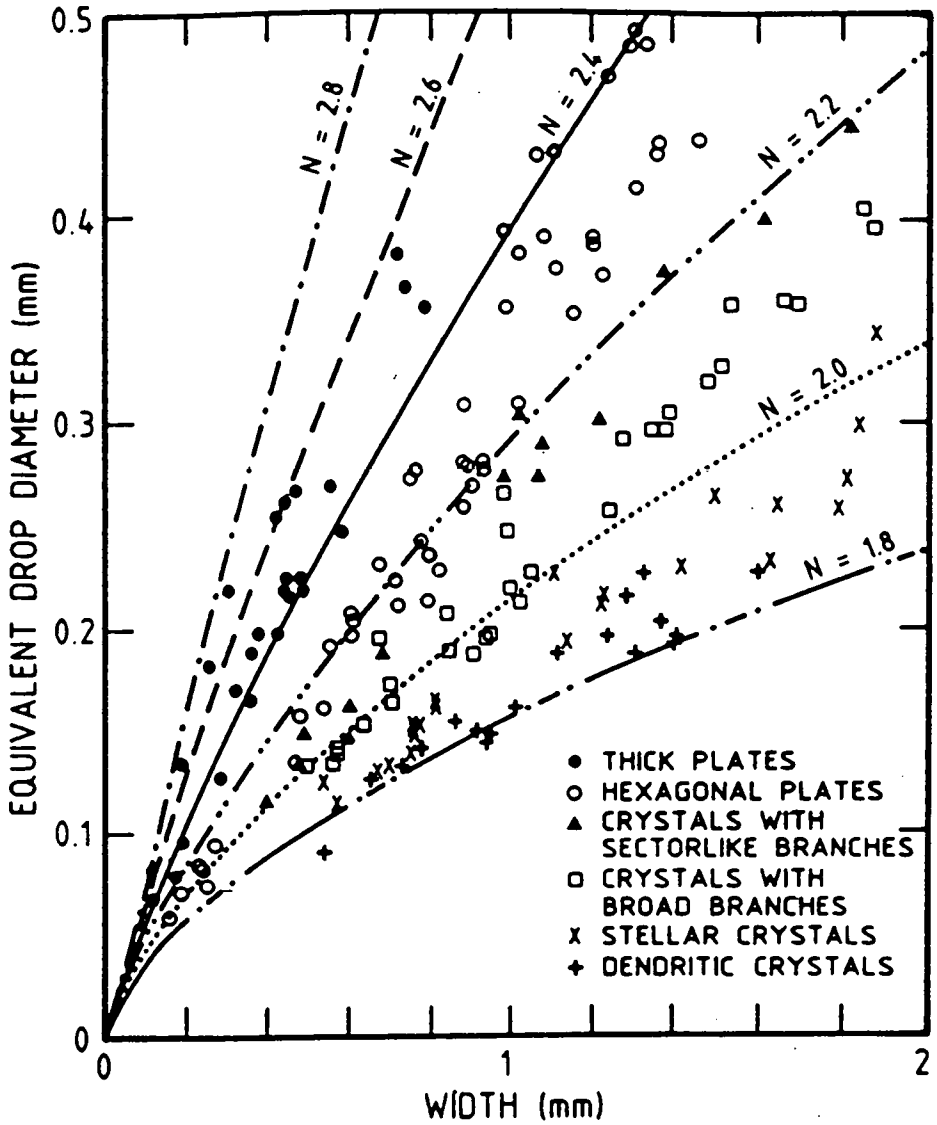

Figure 3. Measurements of the equivalent diameters of drops formed on melting plane form ice crystals measured by Kajikawa [1972] compared with values given by Equation (22) for six values of N.

TABLE 3

CRYSTAL TYPE	N	REFERENCE
Thick Plates	2.4 -2.8	Kajikawa [1972]
Hexagonal Plates	2.2 -2.4	Kajikawa [1972]
Thin Plates	2.1 -2.3	Bashkirova and Pershina [1964]
Plates with sector like Branches	2.1 -2.2	Kajikawa [1972]
Broad Branches	2.0 -2.1	Kajikawa [1972]
Stellar Forms	1.9 -2.0	Kajikawa [1972]
Dendrites	1.75-1.85	Kajikawa [1972]
Stellar Forms	1.7 -2.1	Bashkirova and Pershina [1964]

Equations (17) to (23) above may be combined for the case of no electric field to give the terminal fall velocity to be,

$$U - U_a = \frac{1.34(1 + 2.5\ N_K)}{(1+0.96A_C/A_D)^{0.5})\Sigma_3(\ a_i\ 10^{ci}\ W^{di}\ \rho^{ei}\ \eta^{fi})} (m/s) \quad (24)$$

The values for the coefficients in this expression are given in Table 4

TABLE 4

i	a_i	c_i	d_i	e_i	f_i
1	8.953	11-5.0 N	1 - N	0	1.0
2	5.313	8-3.75N	1-0.75N	0.25	0.5
3	1.813	5-2.5 N	1-0.5 N	0.5	0.0

Figure 4 shows the measured fall velocities of Kajikawa [1972] compared with predictions based on equation (24) for the range of values of N found for plane type ice crystals.

There is much variation in estimates of fall velocities of smaller sized ice crystals. One of the problems that arises with fitting data with power series is that the fitted fall velocities frequently become negative for small crystal widths. Yagi [1970] presented data for the fall velocities of ice crystals whose mean

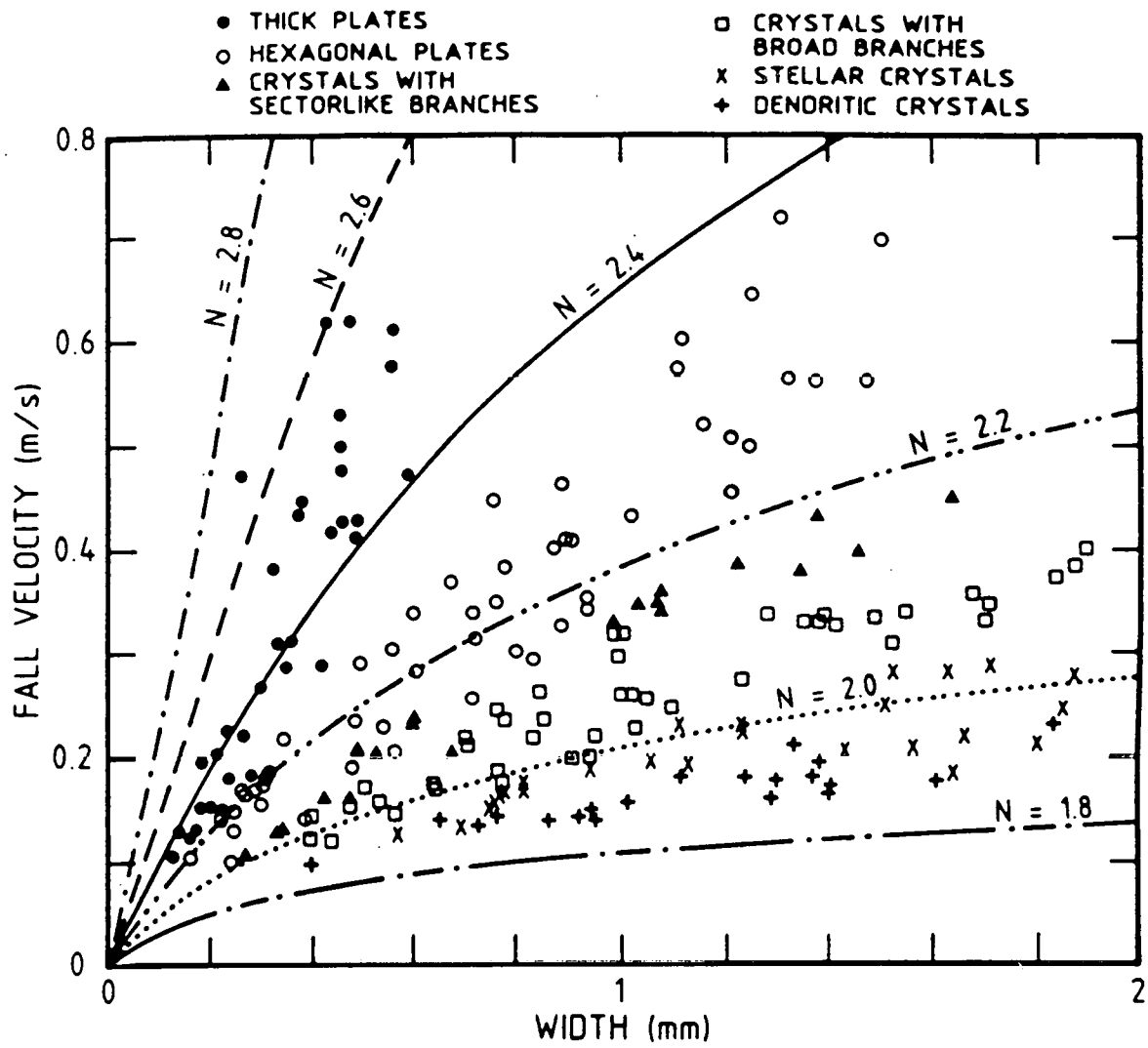

Figure 4. Measurements of the fall velocity of plane form ice crystals measured by Kajikawa [1972] compared with values given by Equation (24) for six values of N.

size was 103 microns drifting in supercooled fog. Figure 5 shows this statistical distribution of velocities compared with values calculated from equation (24) for N = 2.3 assuming the statistical size distribution measured by Yagi [1970].

2.3 COLUMNAR ICE CRYSTALS

Column, bullet, and needle ice crystals have drag coefficients that depend on their length to diameter ratio. Jayaweera and Cottis [1969] made an extensive study of the drag on cylindrical ice crystals. They gave experimental values for the relationship between a modified Davies number X, and the Reynolds number for d/L = 1, 0.5, and 0.1 based on measurements with plastic and aluminum cylinders. For the limiting case as d/L tends to zero, theoretical values from Jayaweera and Mason [1965] were used. Their results are well fitted by the expression,

$$N_R = (1 + 2.5\, N_K)/(b_1\, X^{-1} + b_2\, X^{-0.75} + b_3\, X^{-0.5}) \qquad (25)$$

where
$$b_1 = 3.684 + 13.59\ d/L$$
$$b_2 = 1.299 - 0.8678\ d/L$$
$$b_3 = 0.8311 - 0.04911\ d/L$$

$$X = \left(2\, \rho\, d\, /(L\, \eta^2) \right) F \qquad (26)$$

and
$$N_R = \left(\rho\, d\, /\, \eta \right) \left(U - U_a \right) \qquad (27)$$

Values obtained from equation (25) for the relation of N_R to X are plotted in Figure 6 for four values of d/L. This relation was used for the subsequent analysis of columnar ice crystals.

To calculate the force and the velocity it is necessary to have relationships of the mass and surface area to the crystal length, L. Nakaya and Terada [1935], Bashkirova and Pershina [1964], Ono [1969], Auer and Veal [1970], Heymsfield [1972], Kajikawa [1972], Hobbs et al. [1974], and Locatelli and Hobbs [1974] have studied the masses and dimensions of columnar ice crystals. The density and length to diameter ratio depend on the conditions under which the crystals have grown. Within a given type of crystal general relationships between

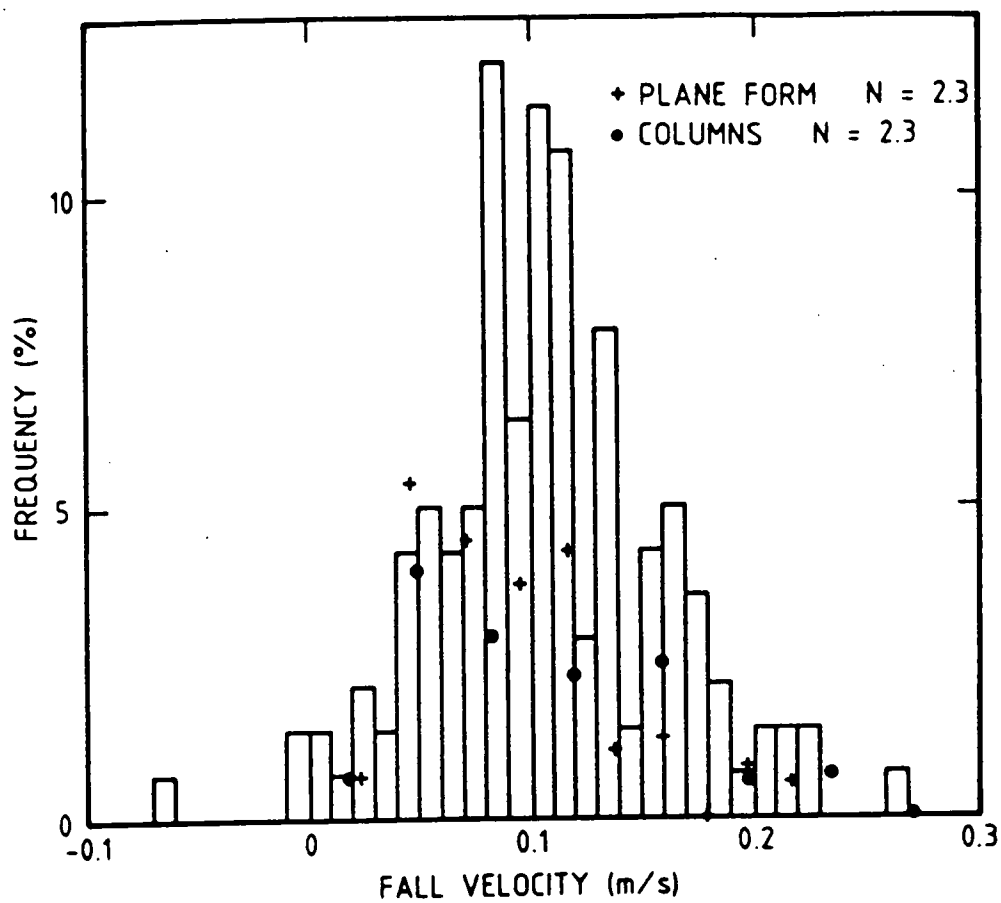

Figure 5. Measurements of the statistical distribution of fall velocities of ice crystals of mean size 103 microns measured by Yagi [1970] compared with values given by Equations (24) and (31) for his size distribution and N = 2.7.

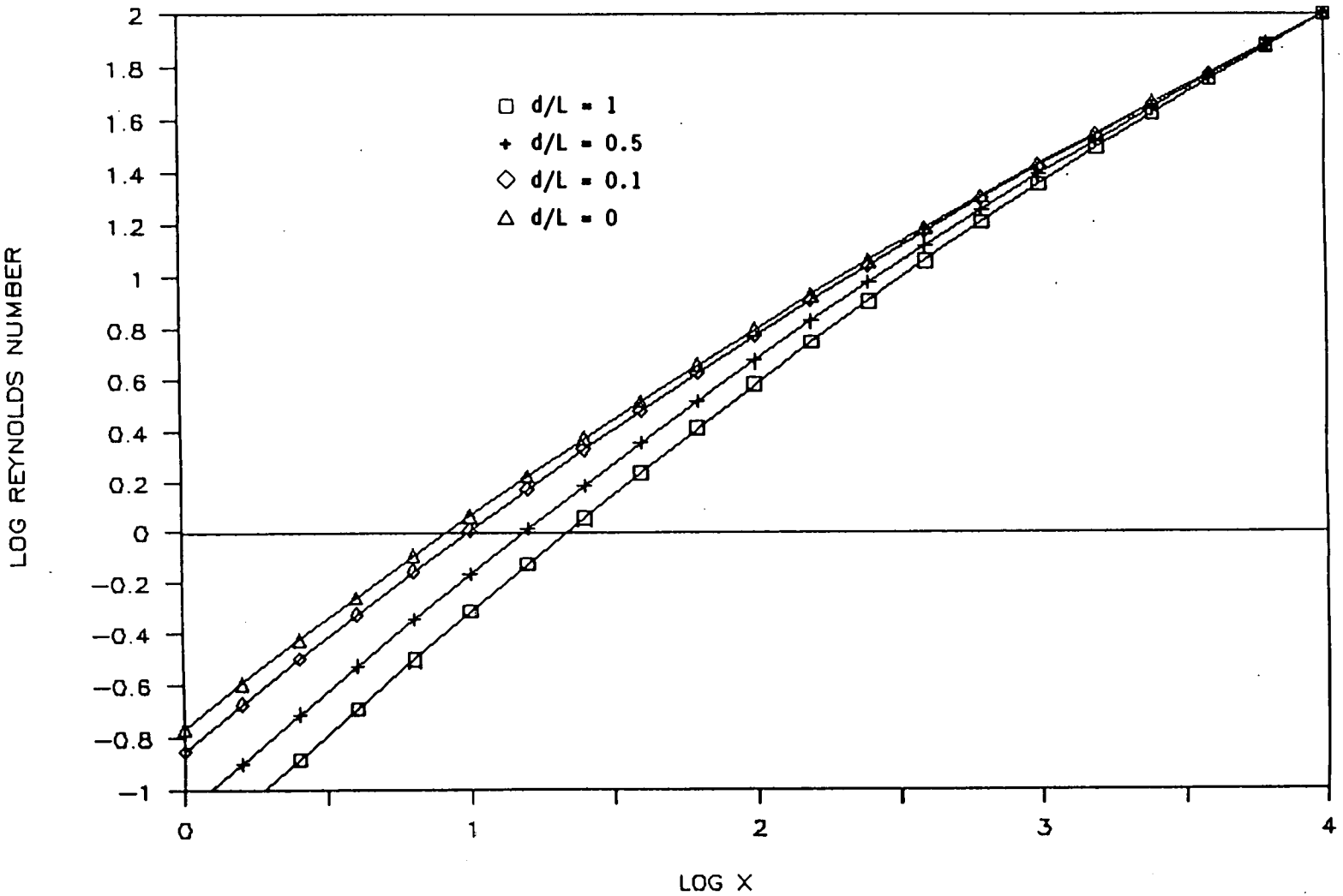

Figure 6. Relationship between the modified Davies number X and the Reynolds number for columns with d/L = 1, 0.5, 0.1 and 0 from Equation (25).

the length, the diameter and the density have been measured but there appears to be considerable scatter.

As with the crystals of plane form it is desirable to have a single parameter which characterizes the crystal size and another which corresponds as far as possible to a given type of crystal. Figure 7 shows measurements of the masses of various types of crystals of columnar form measured by Bashkirova and Pershina [1964]. Superimposed on their data are lines given by the equations,

$$m = m_0 \left(L / d_0 \right)^N \quad \text{(kg)} \qquad (28)$$

where

$$m_0 = \left(\pi \Delta\rho_0 / 6 \right) d_0^3 \quad \text{(kg)} \qquad (29)$$

$$d/L = \left(2 \pi \Delta\rho_0 / 3 \Delta\rho \right) L^{(N-3)/2} d_0^{(3-N)/2} \qquad (30)$$

A value of 10^{-5} m for d_0 and of 1000 (kg/m^3) for $\Delta\rho_0$ have been adopted here because they appear to organize the data well for the smaller diameter-to-length ratio columns in both mass and diameter. They are the same values used for the planar ice crystals. No appreciable improvement in fitting either mass or velocity data was obtained by varying $\Delta\rho_0/\Delta\rho$ from unity so this value was adopted in equation (30). Figure 8 shows the statistical distributions of values of the density exponent N in equation (28) calculated for needle crystals, columns and bullets from the data of Bashkirova and Pershina [1964], for columns for the data of Kajikawa [1972], and for densely rimed columns for the data of Locatelli and Hobbs [1974]. It appears that, as in the case of planar crystals, columnar crystals in the atmosphere have a fairly continuous distribution in N and in size.

Three parameters of columnar ice crystals, the length, N, and C_q, the charge per unit area of surface, are sufficient to calculate the crystal velocities in gravitational and electric fields using equations (25) to (30) in terms of the atmospheric densities. The statistical properties of these parameters can be related to the transport properties of the ensemble of ice crystals.

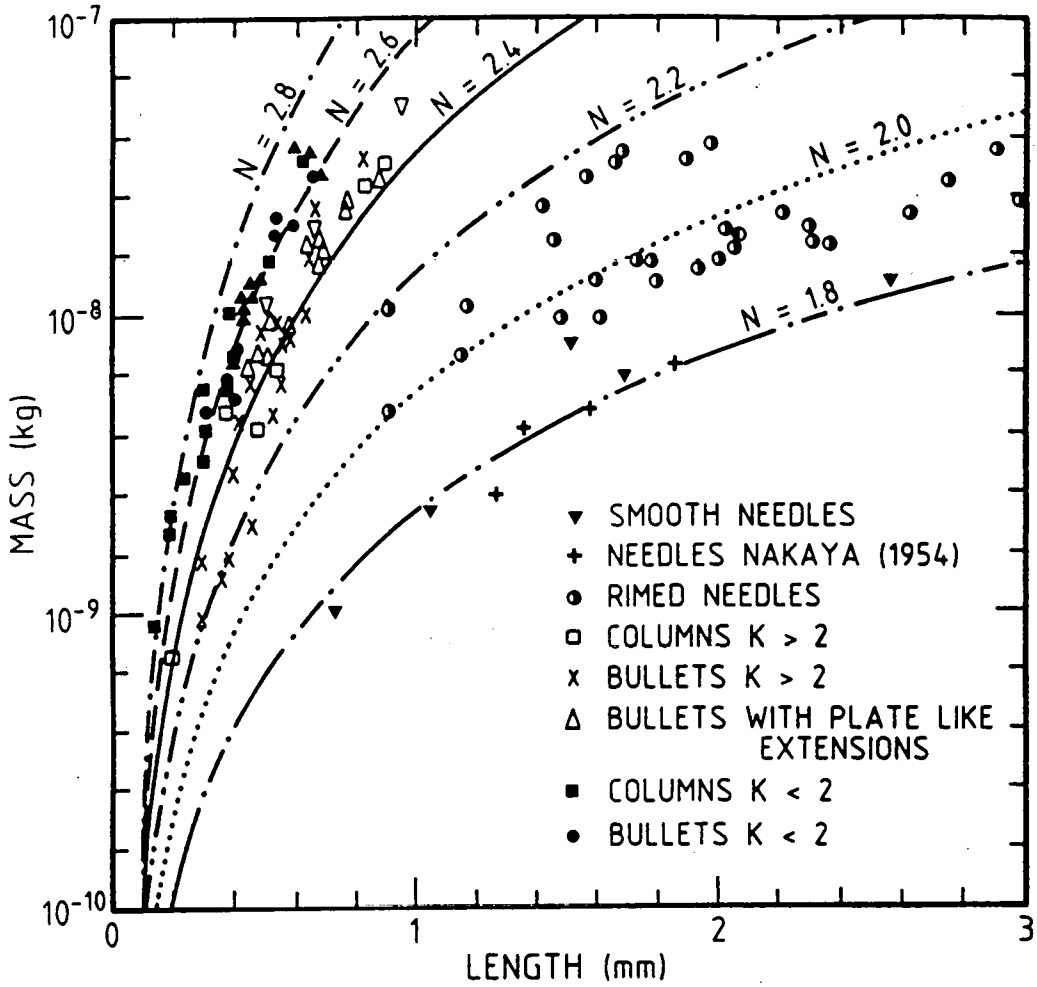

Figure 7. Measurements of the masss of columnar form ice crystals measured by Bashkirova and Pershina [1964] compared with values given by Equation (28) for six values of N.

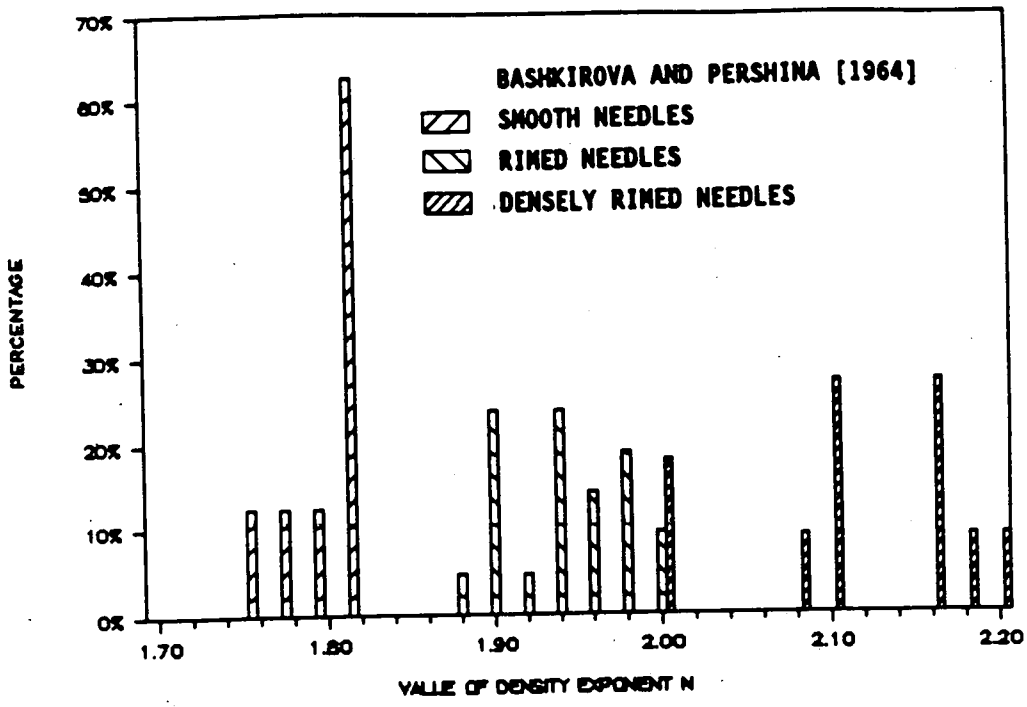

Figure 8a. Measurements of the distribution of masses of needle ice crystals as a function of the parameter N from Equation (28).

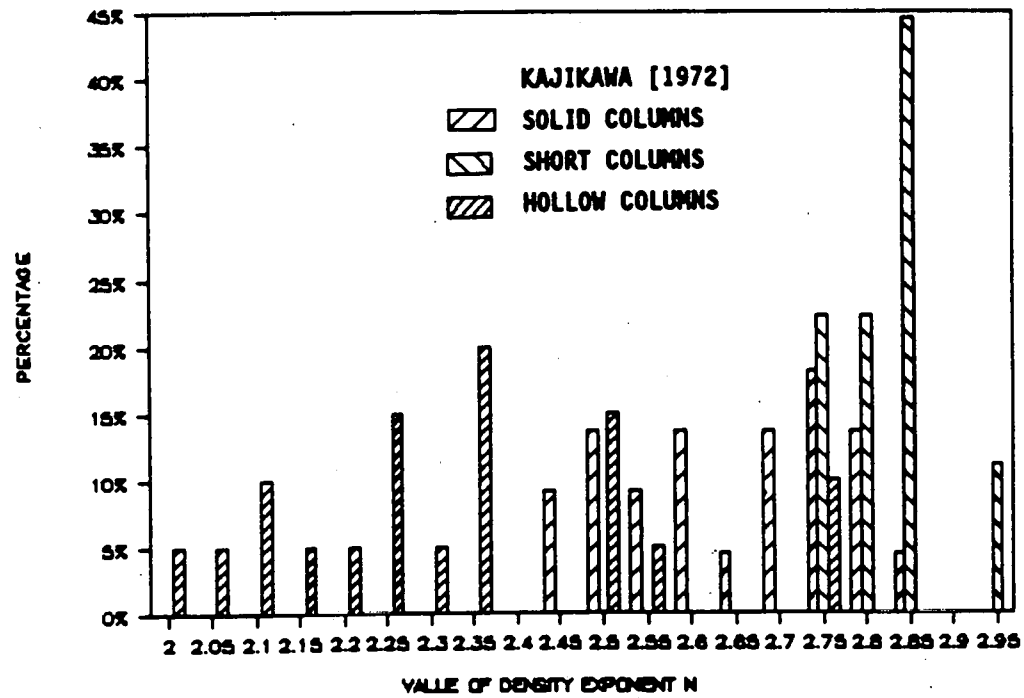

Figure 8b. Measurements of the distribution of masses of columnar ice crystals of as a function of the parameter N.

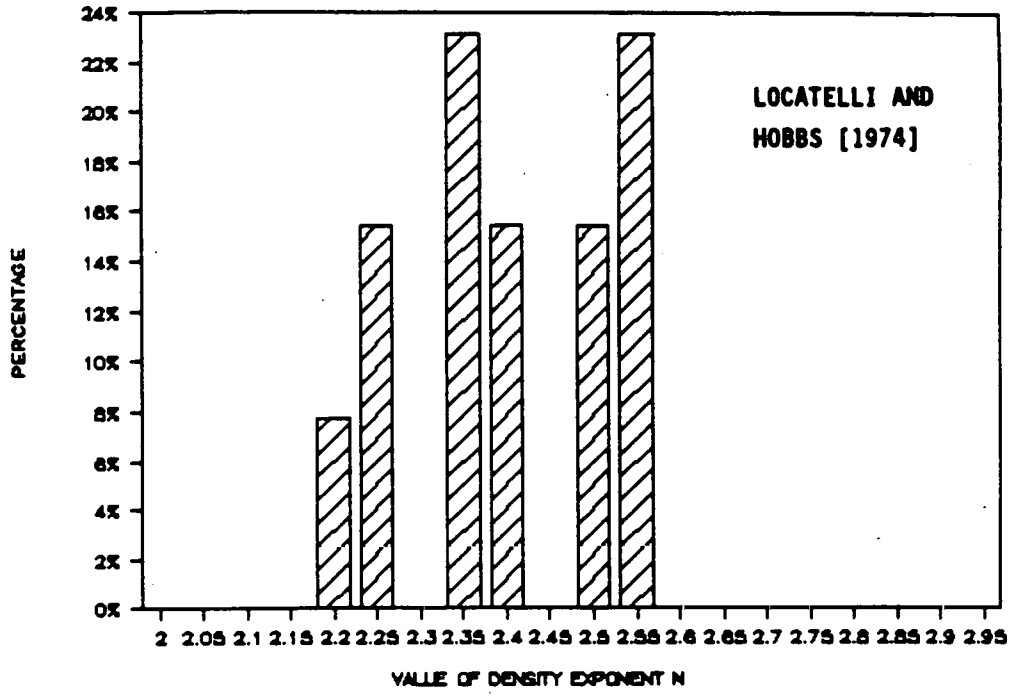

Figure 8c. Measurements of the distribution of masses of densely rimed columns as a function of the parameter N from Equation (28).

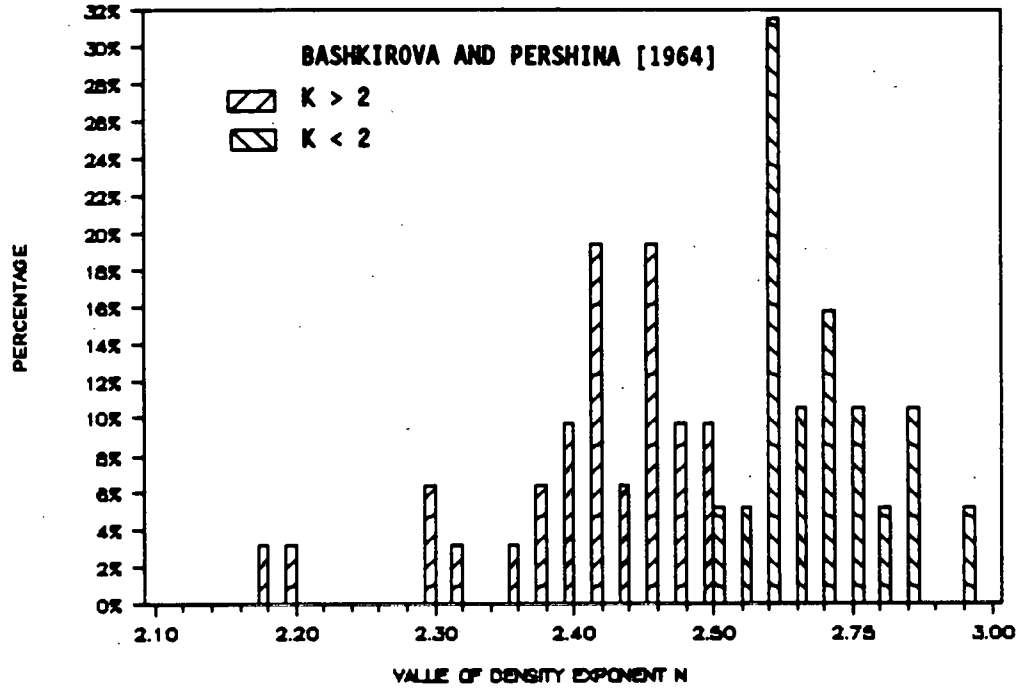

Figure 8d. Measurements of the distribution of masses of column and bullet ice crystals of as a function of the parameter N.

TABLE 5

COLUMN TYPE	N	REFERENCE
Short Columns	2.75-2.95	Kajikawa [1972]
Columns and Bullets K<2	2.5-2.85	Bashkirova and Pershina [1964]
Solid Columns	2.45-2.85	Kajikawa [1972]
Densely Rimed Columns	2.20-2.55	Locatelli and Hobbs [1974]
Columns and Bullets K>2	2.2 - 2.5	Bashkirova and Pershina [1964]
Hollow Columns	2.0-2.55	Kajikawa [1972]
Heavily Rimed Needles	2.0- 2.2	Bashkirova and Pershina [1964]
Rimed Needles	1.88-2.0	Bashkirova and Pershina [1964]
Unrimed Needles	1.76-1.82	Bashkirova and Pershina [1964]

Equations (25) to (30) above may be combined for the case of no electric field to give the terminal fall velocity to be,

$$U-U_a = (1 + 2.5\ N_K)/\Sigma_3(\ a_i\ 10^{ci}\ L^{di}\ \rho^{ei}\ \eta^{fi}\ )(m/s) \quad (31)$$

The values for the coefficients in this expression are given in Table 6

TABLE 6

i	a_i	c_i	d_i	e_i	f_i
1	3.586	11-5.0 N	(1-N)	0	1
2	2.908	6-3.125N	0.625(1-N)	0.25	0.5
3	4.278	1-1.25 N	0.25 (1-N)	0.5	0
4	3.600	4-2.5 N	-0.5 -0.5 N	0	1
5	-5.287	-2-0.625N	-0.875-0.125N	0.25	0.5
6	-6.880	-8+1.25 N	-1.25 +0.25 N	0.5	0

Figure 9 shows the measured fall velocities of Bashkirova and Pershina [1964], Zikmunda and Vali [1972], and Locatelli and Hobbs

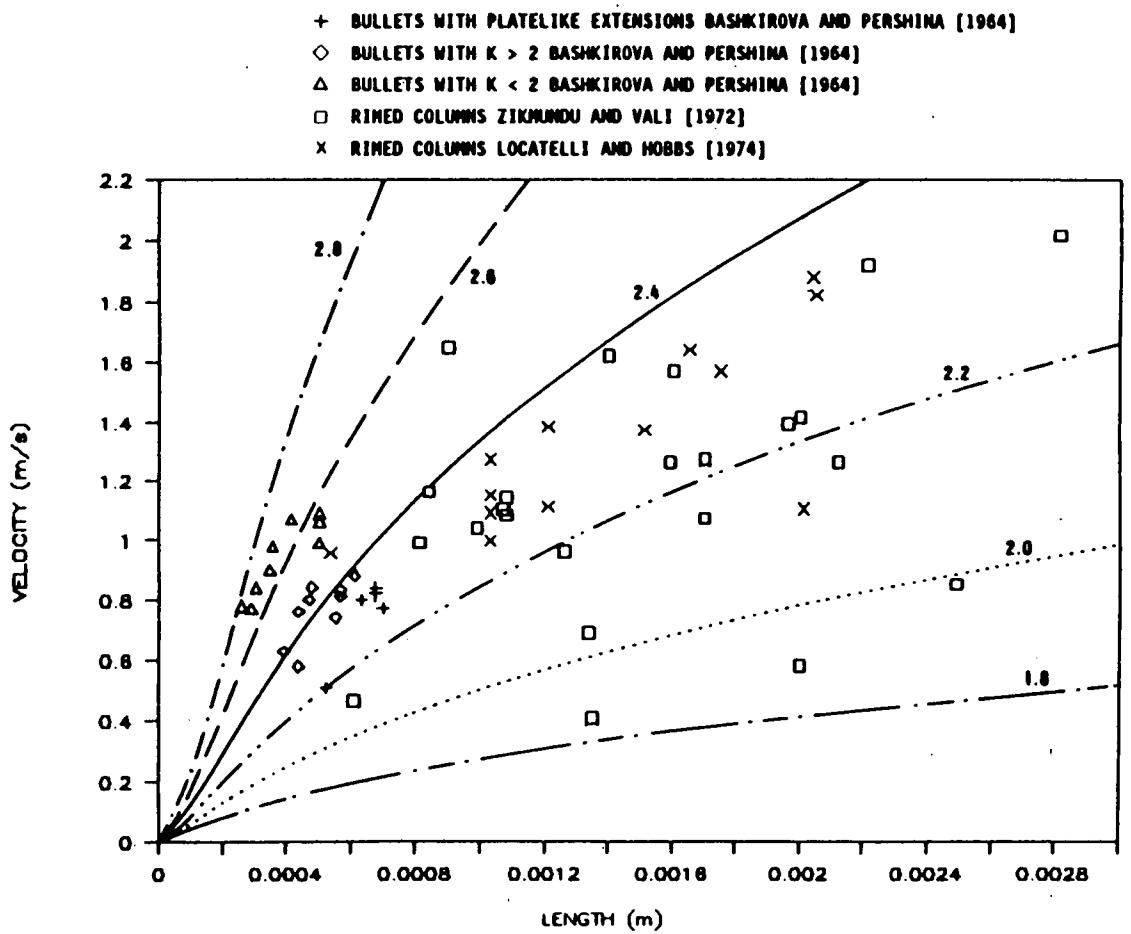

Figure 9. Measurements of the fall velocity of columnar ice crystals measured by Bashkirova and Pershina [1964] Zikmundu and Vali [1972] and Locatelli and Hobbs [1974] compared with values given by Equation (31) for six values of N.

[1974] compared with predictions based on Equation (31) for a range of values of N at a pressure level of 680 mb.

The above treatment depends on the uniformity of the ice crystals and the degree with which they correspond to the models used by Jayaweera and Cottis [1969] so that dynamic similarity can be applied. It is only applicable in the absence of oscillations, rotations, or sideways slips. Crystals of columnar form are particularly sensitive to deviation of the major axis from the horizontal position. Laboratory studies of the fall patterns of unevenly loaded cylinders have shown that these effects can occur, Jayaweera and Mason [1966], Podzimek [1968]. Zikmunda and Vali [1972] have made an extensive study of the fall velocities of rimed ice crystals in natural clouds. Their studies showed that the velocity increases rapidly with increasing angle of deviation and that crystal orientation rapidly became the controlling factor. The terminal velocity increased by about 16% for $g = 20^0$ and by 300-400% for $\alpha = 60\text{-}80^0$. While only a small fraction of the columns observed had large deviations they concluded that as a general rule fall velocities of heavily rimed columns increased by a factor of about two over those of unrimed crystals. The scatter in the fall velocities introduced by riming is evident in the data for 23 rimed columnar crystals from Zikmunda and Vali [1972] shown in Figure 9.

As with other forms of ice crystals several of the published empirical fits to observed velocity distributions give negative drag coefficients for small size crystals. Some of the data for the fall velocities of ice crystals whose mean size was 103 microns drifting in supercooled fog presented by Yagi [1970] concerned those of columnar form. Figure 5 also shows velocities calculated from equation (31) for $N = 2.3$ assuming the statistical size distribution measured by Yagi [1970] compared with measured velocities.

Assemblages of planar and columnar ice crystals are more difficult to treat in a systematic manner than their constituent particles, however, it is important to be able to estimate the effect of aggregation on transport properties. Locatelli and Hobbs [1974] have summarized the range of fall speeds and maximum dimensions for aggregrates and their component particles. Figure 10 has been adapted from Figure 27 of this paper with the addition of the velocities calculated for planar crystals for a range of mass exponents N and a pressure of 680 mb.

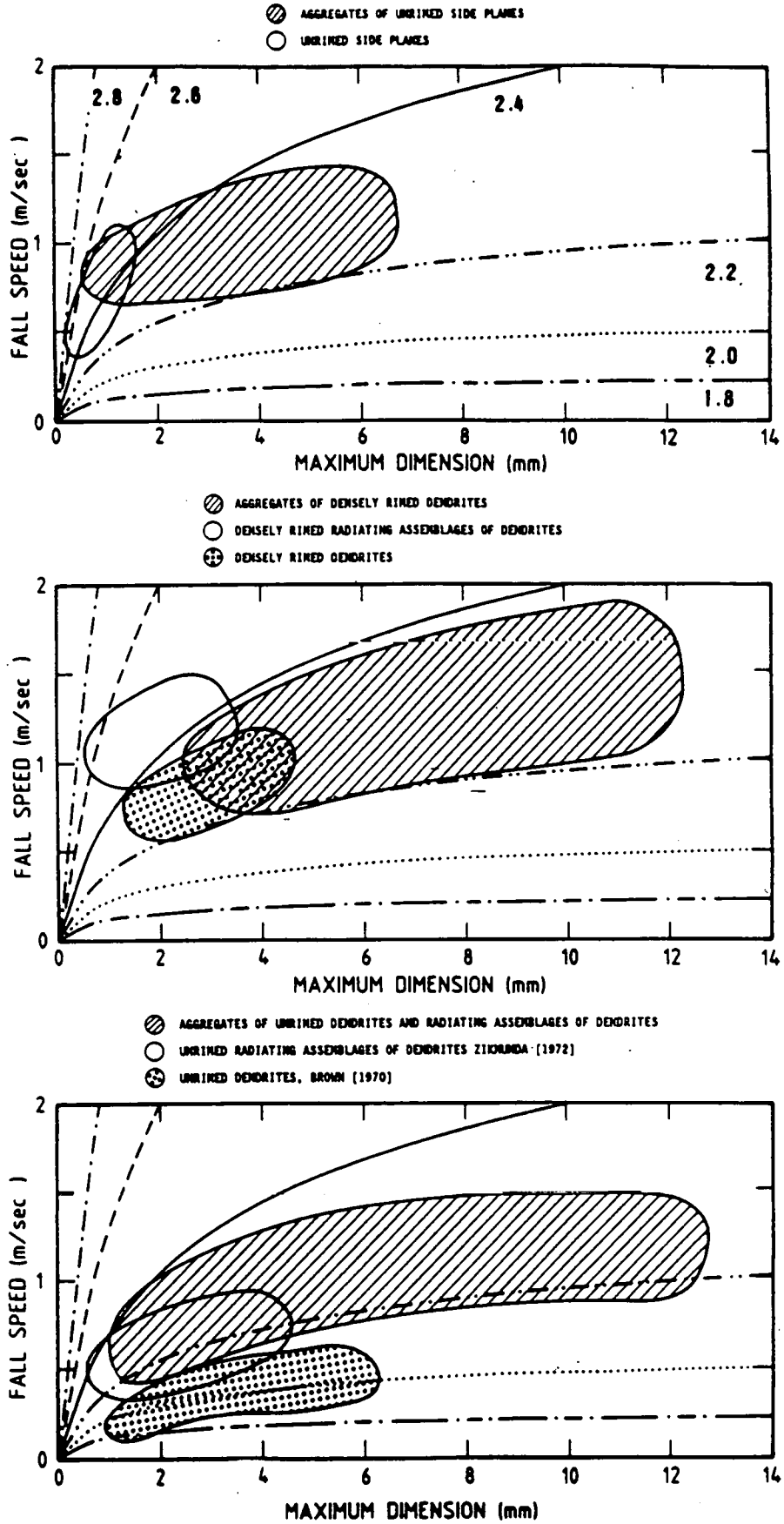

Figure 10. Comparison of the range of fall speeds for aggregrates and their component particles from Locatelli and Hobbs [1974] with velocities from Equation (24) for six values of N.

2.4 CONICAL PARTICLES

List and Schemenauer [1971] have described the sequence of growth by accretion from a dendritic snow crystal to a graupel, then a small hail particle and finally to a hailstone as follows. A dendritic crystal falling in a cloud of supercooled water droplets catches them and becomes filled in, while the total thickness increases. The drag coefficient drops to the disc-like equivalent. Further accretion of cloud droplets will cause the conglomerate to grow in the direction of the vertical axis and a transition is made to the graupel stage with the drag coefficients behaving accordingly. As the particle grows by accretion, heat transfer is less effective, and the accreted water partially enters the ice framework of the graupel, causing densification. This is the small hail stage where tumbling may start; the drag coefficient changes accordingly and eventually the particle falls as a roughly spherical hailstone.

List and Schemenauer [1971] have studied the fall motions of plastic models of conical graupel. The Reynolds number is the sole independent dimensionless parameter to characterize the flow as long as the Navier-Stokes equation describing the situation does not contain a local time derivative, [List 1966]. As soon as the particles do not fall steadily, but oscillate, rotate or move horizontally, then Stroudhal numbers have to be considered. List and Schemenauer [1971] concluded that because such secondary motions were either non-existent or rather small in a majority of their experiments the effect of non-steadiness on their simulations was negligible.

Values of drag coefficient for four conical models were measured by List and Schemenauer [1971]. The four models were,

A a 90° cone-spherical sector,

B a 70° cone-spherical sector,

C a 90° cone-hemisphere,

A a 90° teardrop.

Values of drag coefficient for each of these forms measured when released apex down were used to calculate values of Davies and Reynolds numbers and these were then fitted to the expression,

$$N_R = 1 /(b_1 N_D^{-1}+b_2 N_D^{-0.75}+b_3 N_D^{-0.5}) \qquad (32)$$

Values of these coefficients are listed in Table 7.

TABLE 7

TYPE	H/d	b_1	b_2	b_3	k_1	k_2
A	0.71	37.04	-4.453	1.148	0.219	2.05
B	0.86	64.52	-7.519	1.162	0.288	2.23
C	0.97	51.88	-5.302	1.070	0.376	2.70
D	1.16	42.66	-2.080	0.8309	0.625	4.36

$$N_D = (8 \rho / (\pi \eta^2)) F \qquad (33)$$

where $$F = k_1 \Delta\rho g d^3 + k_2 C_q E d^2 \qquad (34)$$

and $$N_R = (\rho d / \eta) (U - U_a) \qquad (35)$$

Values obtained from equation (32) for the relation of C_d to N_R are plotted in Figure 11 for the four conical forms for comparison with the List and Schemenauer [1971] data.

Equations (32) to (35) above may be combined for the case of no electric field to give the terminal fall velocity to be,

$$U-U_a = 1 / \Sigma_3(a_i \Delta\rho^{ci} d^{di} \rho^{ei} \eta^{fi}) \text{ (m/s)} \qquad (36)$$

The values for the coefficients in this expression are given in Table 8

TABLE 8

	A	B	C	D	SPHERE				
i	ai	ai	ai	ai	ai	ci	di	ei	fi
1	6.771	8.968	5.523	2.732	1.666	-1.00	-2.00	0.00	1.00
2	-1.245	-1.712	-0.988	-0.265	0.347	-0.75	-1.25	0.25	0.50
3	0.491	0.433	0.349	0.210	0.155	-0.50	-0.50	0.50	0.00

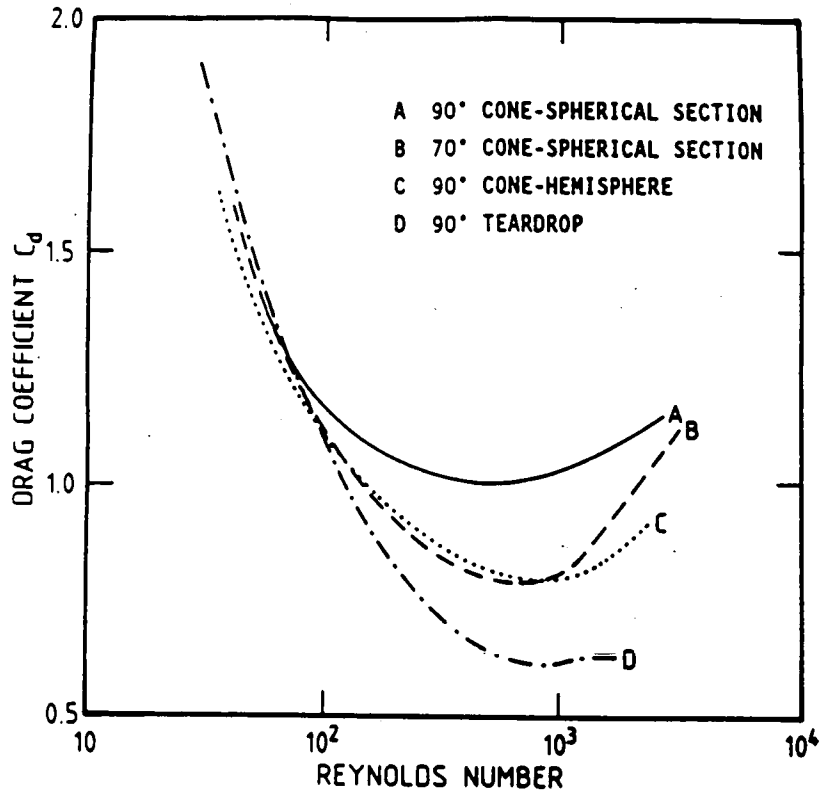

Figure 11a. Values of C_d for four conical crystal forms from List and Schemenauer (1971].

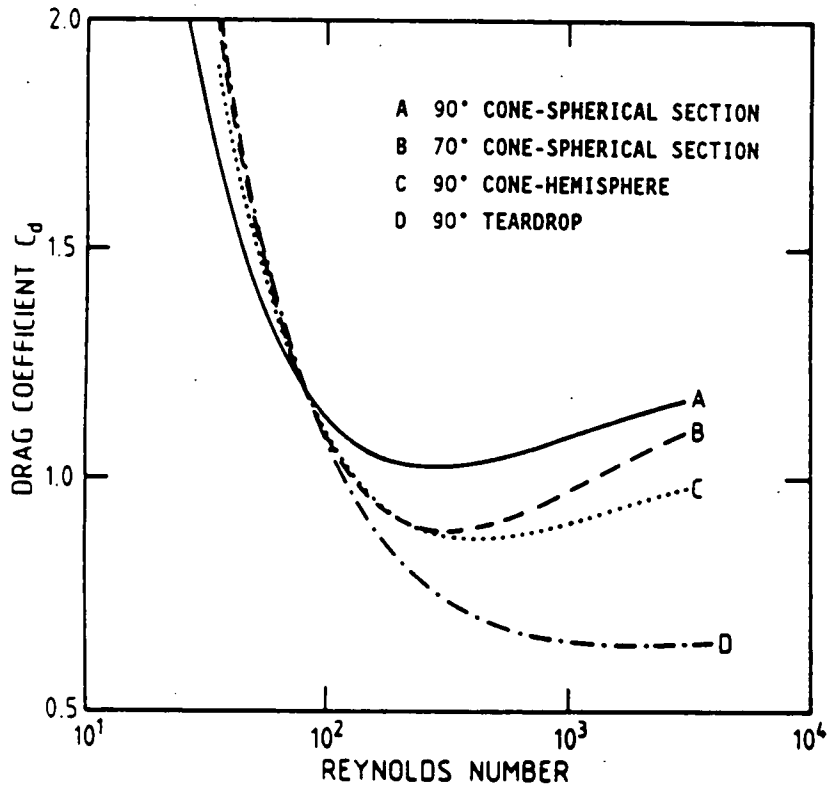

Figure 11b. Values of C_d derived from Equation (32) for the same four conical crystal forms.

2.5 WATER DROPS AND DROPLETS

Small water drops are spherical and the treatment given in Section 2.1 is applicable. Water drops above a diameter of about 0.5 mm become nonspherical, and both the cross sectional area in the horizontal plane and the drag coefficient are greater than for spherical particles of the same mass and equivalent diameter. These effects have been experimentally studied by Lenard [1904], Flower [1928], Laws [1941], Gunn and Kinzer [1949], Blanchard [1950, 1955], Kumai and Itagaki [1954], Magono [1954], Jones [1959], Pruppacher and Beard [1970], and Pruppacher and Pitter [1971]. Empirical relations for the velocity as a function of drop size of various ranges of application and complexity have been given by Best [1950], Liu and Orville [1969], Ogura and Takahashi [1973], Berry and Pranger [1974], Beard [1976], Shiino [1983], and Liu [1986].

When fall velocities of only uncharged water drops are concerned it may be adequate to use a unique analytic relationship between d and the axial ratio of the drop b/a as was done by Beard [1976]. The temperature dependence of the surface tension is not very important and the pressure on the surface, because it is only controlled by the mass of the water drop, remains constant with height. This assumption is not valid for mobility calculations because the force, and hence the drop shape, depend on the electric field.

Green [1975] has developed a simple analytic model which assumes that the drop shape approximates that of an oblate spheroid for all deformations and which determines the equilibrium shape by considering only the hydrostatic and surface tension stresses. This approximation appears to be justified by a more complete analysis by Pitter and Pruppacher [Pruppacher and Klett; 1978, p315] which showed that dynamic stresses cause only weak to moderate distortions in the shape of an oblate spheroid. The aspect ratios and maximum diameters given by Green [1975] agree well with the experimental results of Pruppacher and Pitter [1971].

The analytic expression of Green [1975] may be written,

$$N_{Bo} = 4\ (a/b)^{1/3}\ [(a/b)^2 - 2\ (a/b)^{1/3} + 1\ ] \qquad (36)$$

where the Bond number, a nondimensional parameter relating the pressure on the surface to the surface tension is given by,

$$N_{Bo} = 6 F / (\pi d \sigma) \qquad (37)$$

a/b = the ratio of the major diameter to the height

$d = a^{2/3} b^{1/3}$ is the equivalent drop diameter.

and σ is the surface tension of water with respect to air.

Equation (36) is not in a convenient form for the calculation of a/b from the Bond number. It may, however, be fitted by the expression,

$$a/b = 1 + 0.1472 N_{Bo}^{0.8} \qquad (38)$$

Values of b/a calculated from equation (38) are shown in Figure 12 compared with experimental values of Pruppacher and Pitter [1971]. This function can be used to relate the drop shape to the force on the particle.

Two effects occur due to the deformation of the shape of the drops. The cross sectional area normal to the flow direction increases and the drag coefficient increases, Maklin and Ludlam [1961]. It is apparent, however, that large departures from a spherical form do not take place until the drop diameter has reached about 0.5 mm. By this time the Reynolds numbers are already large enough that the ratio of the drag coefficients of spherical to ellipsoidal particles is not greatly dependent on Reynolds number. It thus appears that a simple relation can be used to relate the drag coefficient to the value of a/b.

The relation given in equation (12) for spherical particles can thus be used to relate the Davies number to the force and the effects of drop deformation included by modifying the relation between the calculated Reynolds number and the velocity.

$$N_R = (1 + 2.5 N_K)/(b_1 N_D^{-1} + b_2 N_D^{-0.75} + b_3 N_D^{-0.5}) \qquad (39)$$

where, $b_1 = 21.786$

$b_2 = 2.3836$

$b_3 = 0.5590$

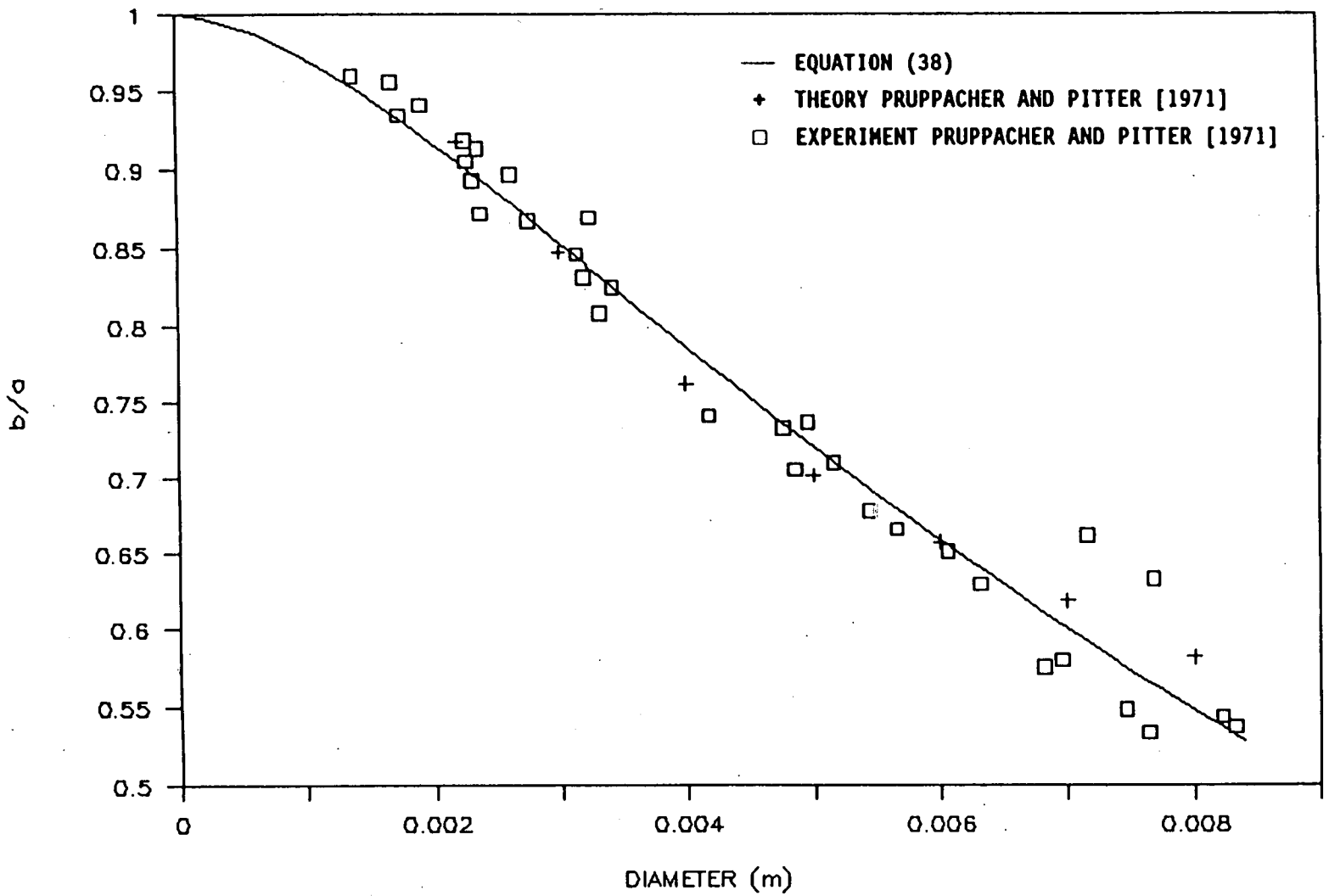

Figure 12. Values of b/a, the ratio of the height to the diameter in the horisontal plane from Equation (38) compared with theoretical and experimental values from Pruppacher and Pitter [1971].

$$N_D = 8 \rho / \eta^2 [(g \Delta\rho/6)d^3 + E C_q d^2] \quad (40)$$

and $U - U_a = (\eta / \rho d) N_R (a/b)^{-0.75}$ (41)

with $a/b = 1 + 0.1472 N_{Bo}^{0.8}$ (38)

where $N_{Bo} = [g \Delta\rho d^2 + 6 E C_q d] / \sigma$ (42)

Figure 13 shows the fall velocities for water drops given by Equation (41) compared with the measurements of Gunn and Kinzer [1949] and the empirical models of Liu and Orville [1969], Manton and Cotton [1979], Shiino [1983], and Liu [1986]. The agreement between equation (41) and the experimental results is quite satisfactory at the larger drop sizes where the effects of drop shape become important. Differences with the Gunn and Kinzer [1949] data are evident for the smaller particles, however, Beard and Pruppacher [1969] concluded that their results were in error in this region due to evaporation. In this size range the drops are spherical and equation (41) gives essentially the same results as equation (16) which has been compared with the relations given by Beard [1976] for the size range up to 20 micro m in Figure 1 and the relations of LeClair et al. [1970], Beard and Pruppacher [1969], and Perry [1950] in Figure 2. Beard [1976] gives three relationships for water drop velocities according to size range. His relationship for the size range 19 micro m and 1.07 mm is essentially identical to those of LeClair et al. [1970], Beard and Pruppacher [1969], and Perry [1950] and between 1.07 mm and 7 mm is essentially identical to the Gunn and Kinzer [1949] data. Equation (41) should thus give adequate values for water drop velocities in gravitational and electric fields for any atmospheric conditions over the size range from 0.5 micro m to 7 mm.

3. SEDIMENTATION VELOCITIES AND MOBILITIES

While the relations given in Section 2 are quite simple they involve the calculation of the Davies numbers from the diameters, densities, viscosities, and electric fields, and the velocities from the Reynolds numbers, densities and viscosities. It is convenient to have simple expressions for the sedimentation velocity and mobility

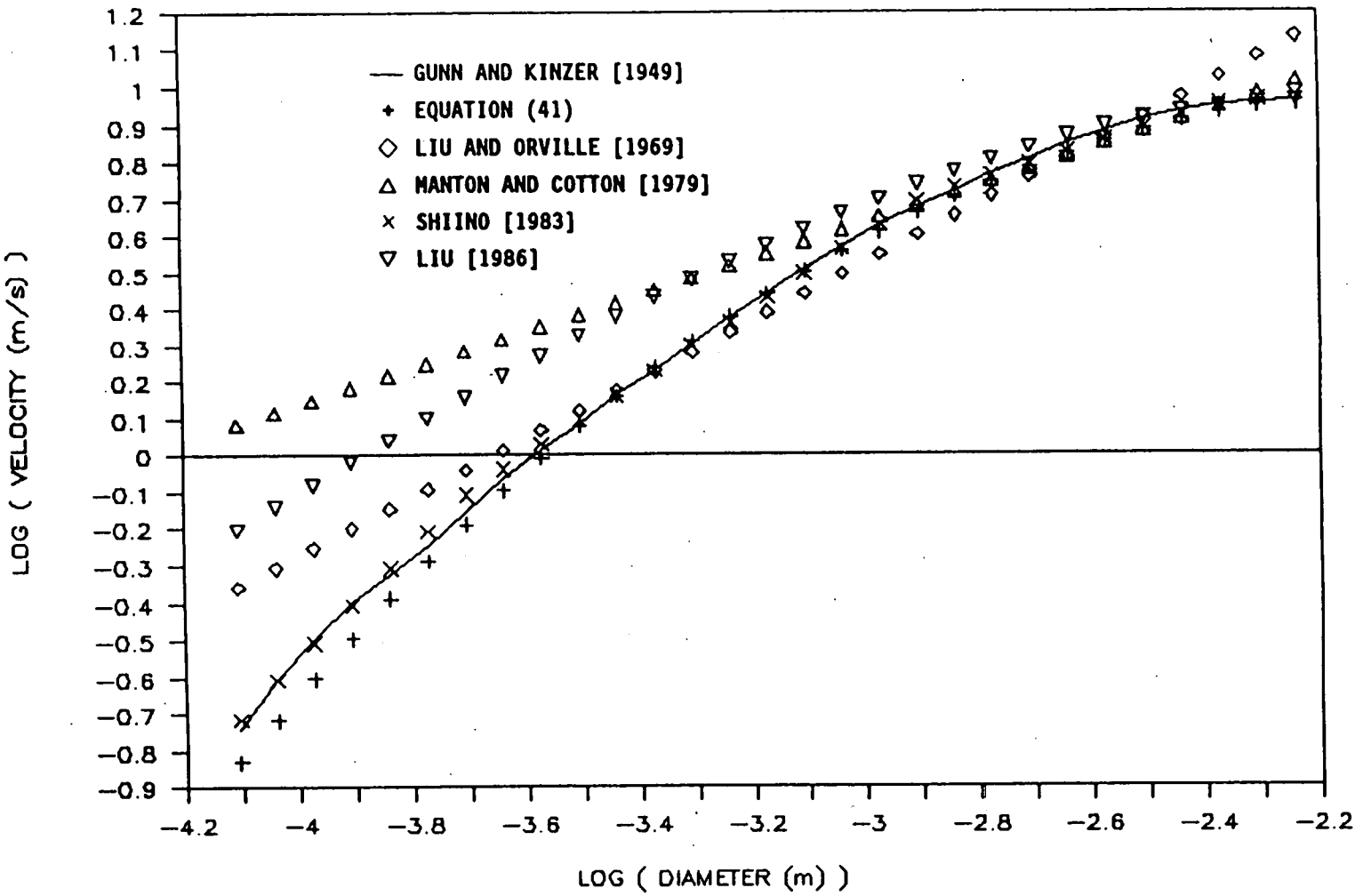

Figure 13. Fall velocities for water drops given by Equation (41) compared with the measurements of Gunn and Kinzer [1949] and equations of Liu and Orville [1969], Manton and Cotton [1979], Shiino [1983], and Liu [1986].

in terms of the particle diameter, particle density, and the ambient atmospheric pressure. Such relations are useful, for example, when making estimates of the relative importance of electric fields, crystal size or habit. The simplicity of the expressions can also provide important savings in large computer programs.

Before using mobilities to relate the velocity to the electric field for drop sized particles it is important to determine the validity of the concept. For particles in the Stokes' drag regime the velocity is proportional to the force and hence to the electric field. For larger particles, however, the velocity is proportional to the square root of the total force on the particle. The linearity of the process thus depends on the fraction of the force provided by the electric field. Takahashi [1973] has summarized measured values of charge on cloud drops up through precipitation particles. These data show that larger values of the charge per unit surface area in thunderstorm clouds can be approximately represented by $C_q = 5\ 10^{-7}$ C m^{-2}. Gunn [1949] using aircraft measured mean maximum electric field strengths of $1.3\ 10^5$ V m^{-1} and on once an electric field of $3.4\ 10^5$ V m^{-1} just before the aircraft was struck. Fitzgerald and Byers [1962] measured fields as large as $2.3\ 10^5$ V m^{-1}, and Holitza and Kasemir [1974] as large as $3\ 10^5$ V m^{-2}. Winn et al. [1974] measured peak values in excess of $1\ 10^5$ V m^{-1} 10% of the time and once observed a field as large as $4\ 10^5$ V m^{-1}. It would thus appear that a typical large value for C_q E, the product of the charge per unit surface area and the electric field, might be about $5\ 10^{-2}$ J m^{-3} with maximum values as large as $2\ 10^{-1}$ J m^{-3}. Figure (14) shows the normalized mobilities for spherical particles calculated using Equation (12) for three values of C_q E. Figure (15) shows the mobilities for planar ice crystals with N = 2 calculated using Equation (24) and Figure (16) the values for columnar ice crystals using Equation (25) again for the same three values of C_q E. It would thus appear that for reasonable values of C_q E the use of estimates based on the assumption of an electric field independent mobility should provide a good estimate of the velocity components produced by the electric fields. In cases where the electric and gravitational forces are approximately equal and opposite the use of the expressions given in Section 2 in terms of the Davies numbers is, of course, advisable.

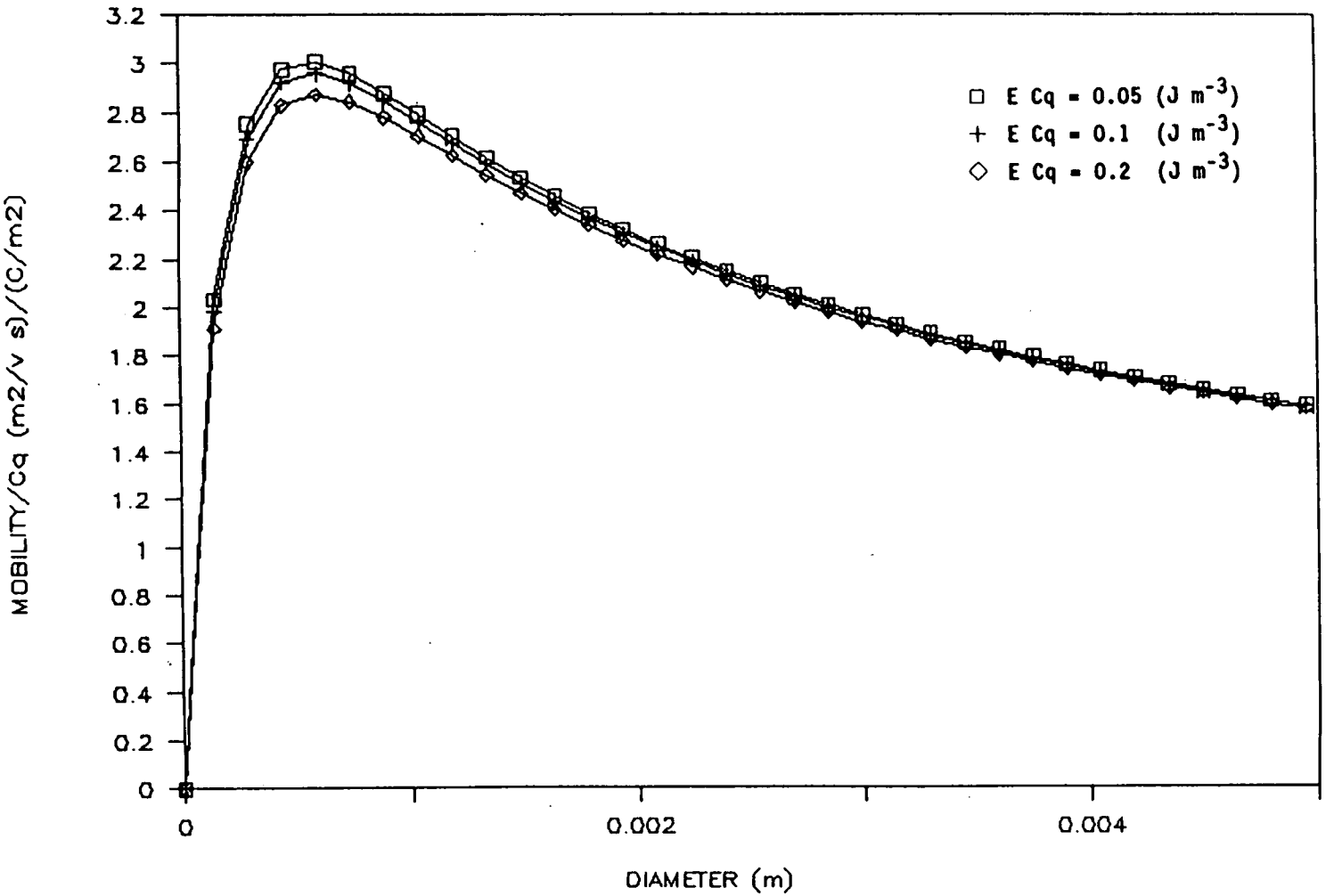

Figure 14. Mobilities for spherical ice crystals for Cq E = 0.05, 0.1, and 0.2 (J m^{-3})

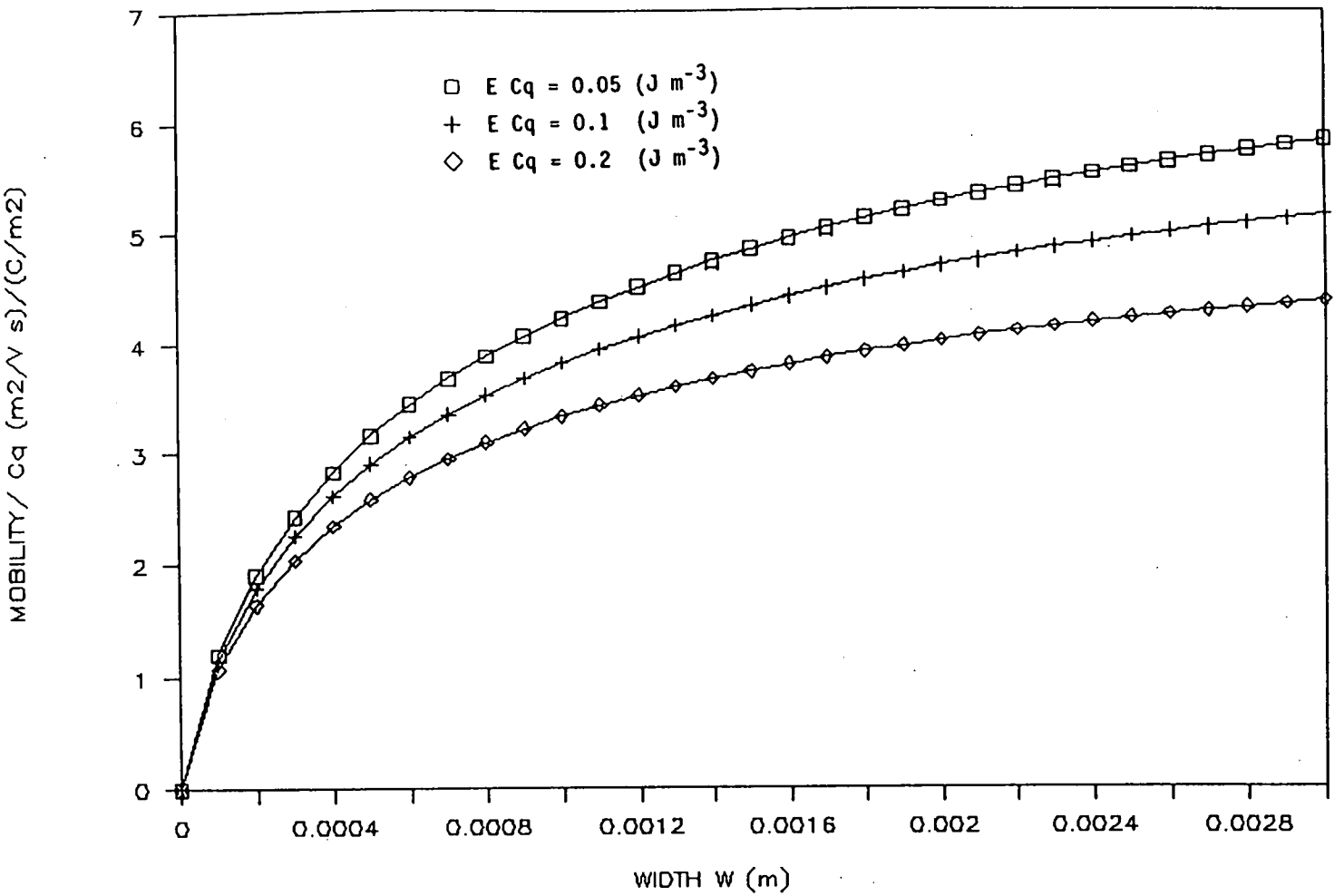

Figure 15. Mobilities for planar ice crystals of M = 2.2 for Cq E = 0.05, 0.1, and 0.2 (J m^{-3})

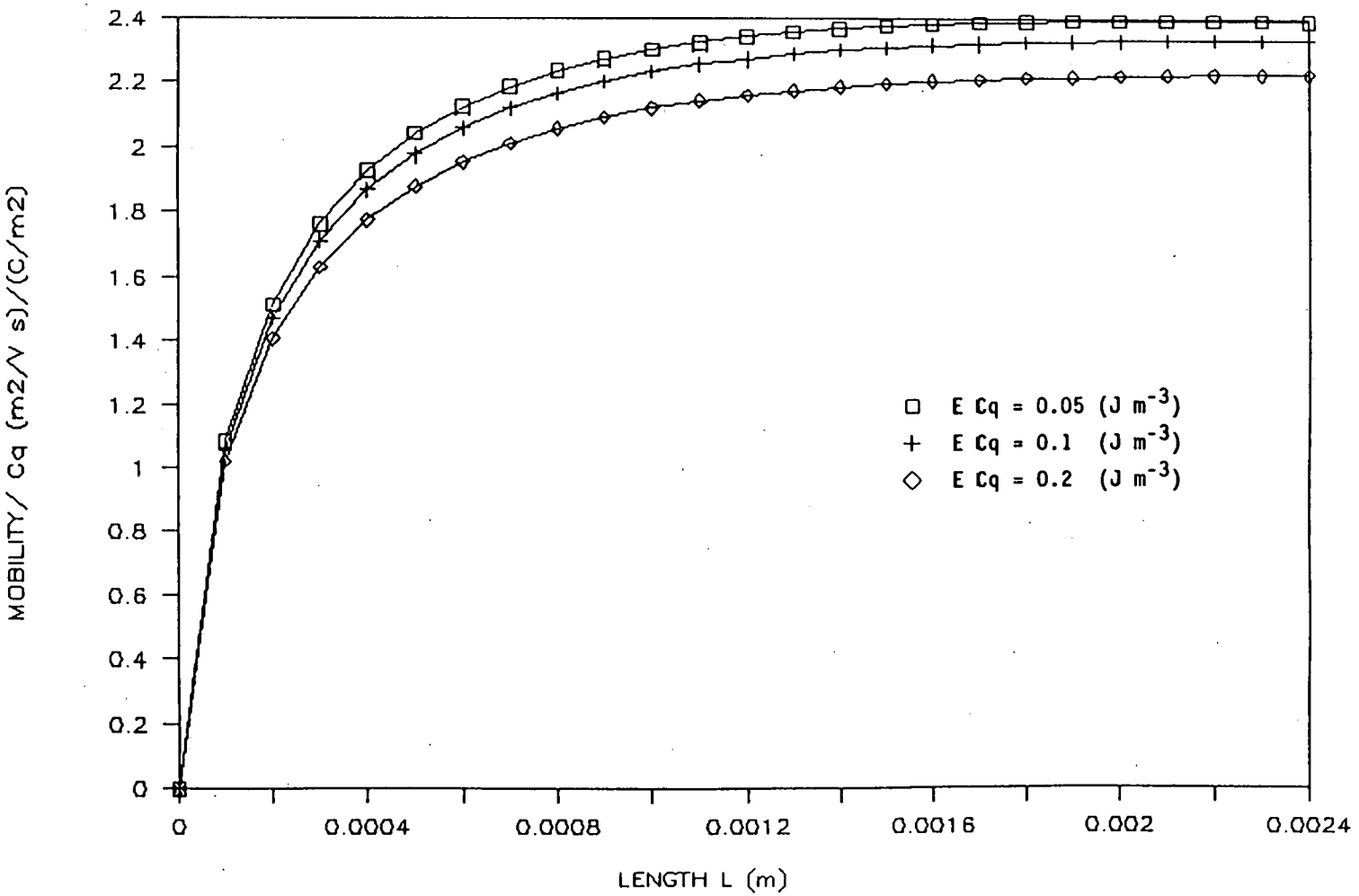

Figure 16 Mobilities for columnar ice crystals of N = 2.2 for Cq E = 0.05, 0.1, and 0.2 (J m^{-3})

3.1 SPHERES

The expression for the velocity obtained by fitting equation (16) is,

$$U - U_a = 1 / \Sigma_3 \left(a_i \, \Delta\rho^{ji} \, p^{ki} \, d^{li} \right) \text{ (m/s)} \qquad (43)$$

The values for the coefficients in this expression are given in Table 9

TABLE 9

i	a_i	j_i	k_i	l_i
1	3.079E-5	-1.000	0.1522	-2.00
2	1.548E-3	-0.750	0.2790	-1.25
3	1.668E-1	-0.500	0.4057	-0.50

and for the mobility is,

$$B = C_q / \Sigma_3 \left(b_i \, \Delta\rho^{mi} \, p^{ni} \, d^{oi} \right) \text{ (m}^2\text{/V s)} \qquad (44)$$

The values for the coefficients in this expression are given in Table 10 .

TABLE 10

i	b_i	m_i	n_i	o_i
1	3.440E-5	0.0670	0.1522	-1.0
2	2.810E-3	0.1606	0.2790	-0.25
3	5.234E-1	0.5051	0.4057	+0.5

where $\Delta\rho$ is the particle density (kg/m^3)
and p is the pressure (bar) , 1 N/m^2 = 10^{-5} bar

The US Standard Atmosphere [1976] was used to relate the temperature and viscosity to the pressure. The calculated sedimentation velocity of a 1 mm diameter particle with a density of 1000 kg/m3 at the 0.4 bar level changed by only 2% between using the 30 N July and the 75 N January (Cold) US Standard Atmosphere [1966] models.

Figure (17) shows values of the velocity as a function of the particle diameter for six different altitudes and Figure (18) shows the corresponding mobility normalized by dividing by C_q. Figures (19) and (20) show the corresponding relations at three values of particle density.

3.2 PLANE FORM CRYSTALS

Using the relationships given in Section 2.2 equations can been derived for the velocities and mobilities as functions of N, the crystal width, and the pressure.

$$U - U_a = 1 / \Sigma_3 (a_i 10^{ji} W^{ki} p^{li}) \quad (m/s) \qquad (45)$$

The values for the coefficients in this expression are given in Table 11

TABLE 11

i	a_i	j_i	k_i	l_i
1	9.016	6-4.905 N	1 - N	0.1522
2	1.291	6-3.655 N	1-0.75N	0.2790
3	1.064	5-2.405 N	1-0.5 N	0.4057

$$B = C_q / \Sigma_3 (b_i 10^{mi} W^{ni} p^{oi}) \quad (m^2/V\ s) \qquad (46)$$

The values for the coefficients in this expression are given in Table 12

TABLE 12

i	b_i	m_i	n_i	o_i
1	$0.5944+192.2\ N^{-7.2}$	-4	-1.0	0.1522
2	$0.4421+151.4\ N^{-7.7}$	0	0	0.2790
3	$-585.0+0.9020\ N^{+7.7}$	-2	+0.5	0.4057

Plots of the sedimentation velocities of plane form ice crystals at the 400 mb level for a range of values of N are given in Figure 21 and the corresponding normalized mobilities are shown in Figure 22. Plots of the fall velocities at several different

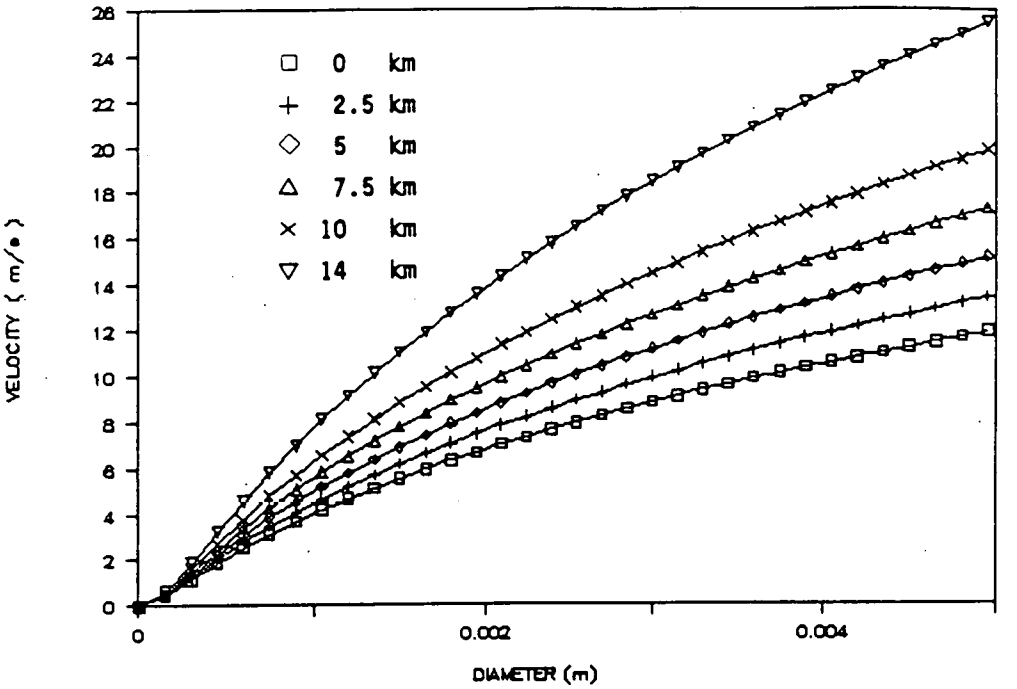

Figure 17. Fall velocities of spherical particles with particle densities of 1000 kg/m^3 at 0, 2.5, 5, 7.5, 10, and 14 km.

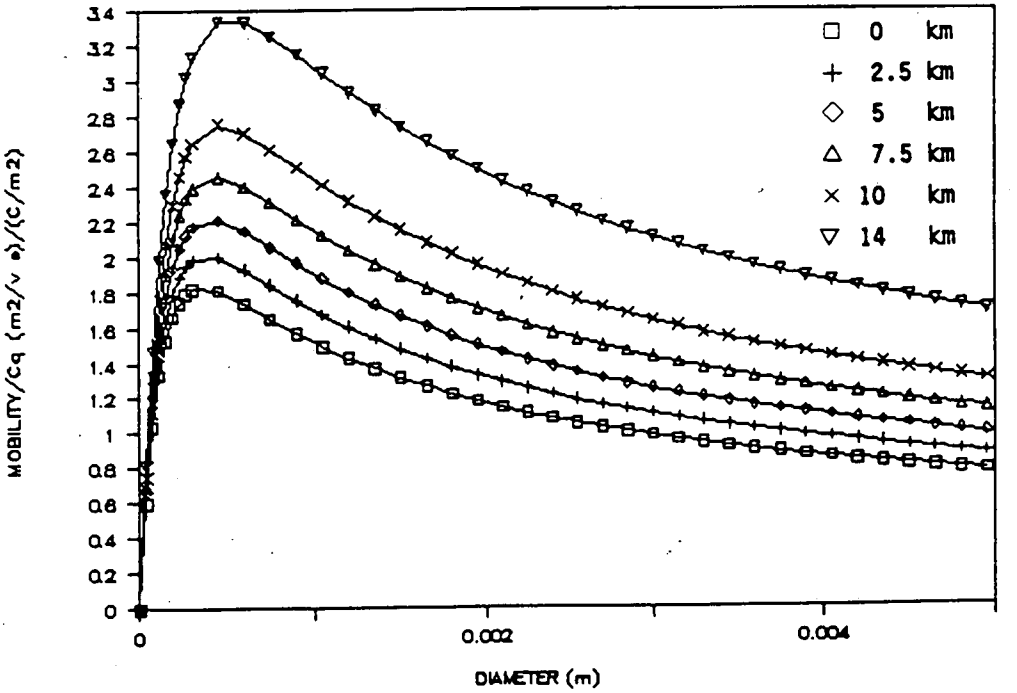

Figure 18. Mobilities of spherical particles with particle densities of 1000 kg/m^3 at 0, 2.5, 5, 7.5, 10, and 14 km.

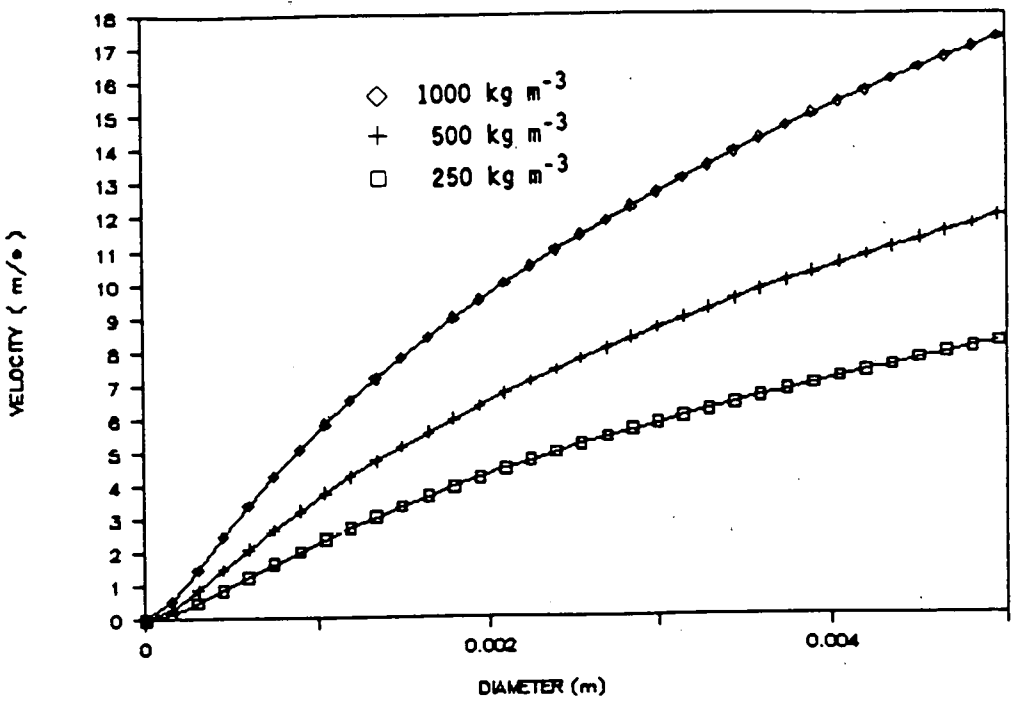

Figure 19. Fall velocities of spherical particles at the 400 mb level for particle densities of 1000, 500, and 250 kg/m^3.

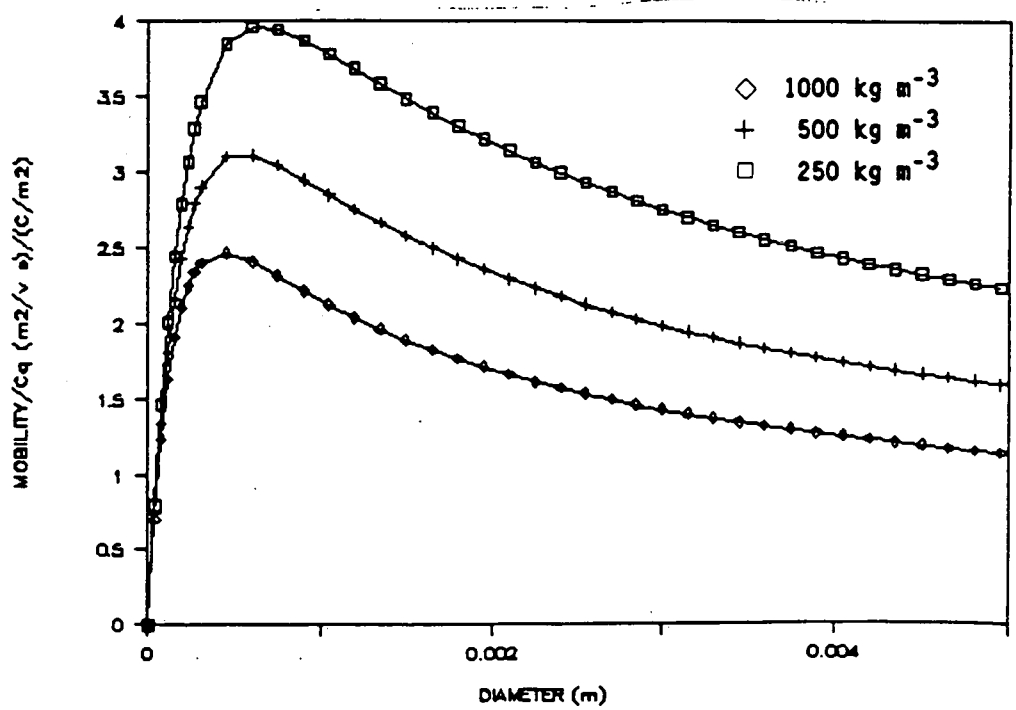

Figure 20. Mobilities of spherical particles at the 400 mb level for particle densities of 1000, 500, and 250 kg/m^3.

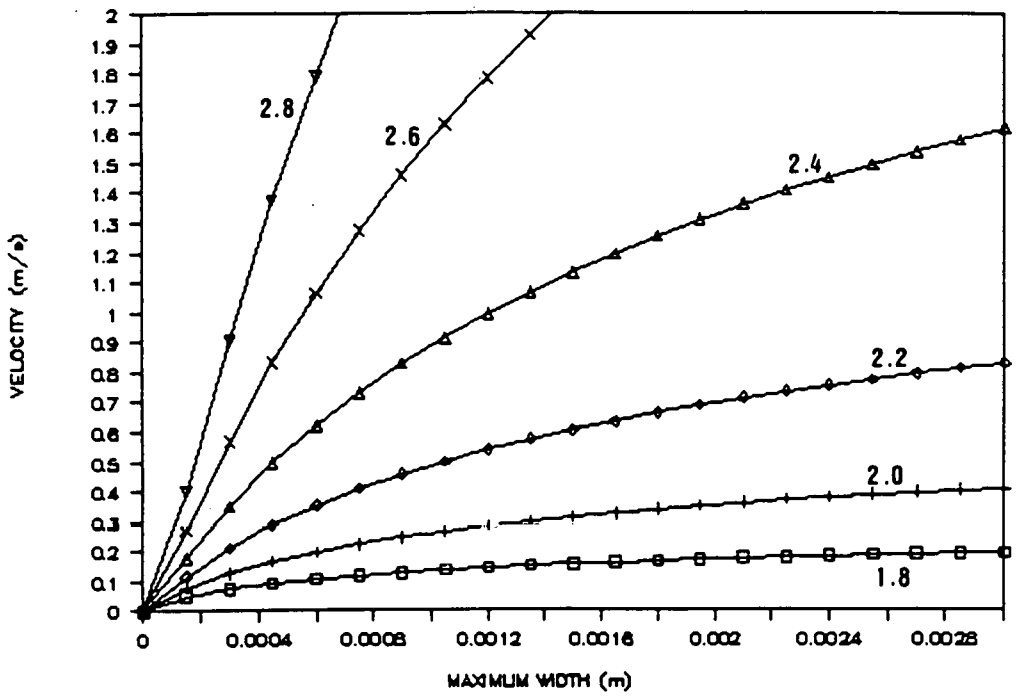

Figure 21. Fall velocities of plane form ice crystals at the 400 mb level for values of density exponent N of 1.8, 2, 2.2, 2.4 and 2.8.

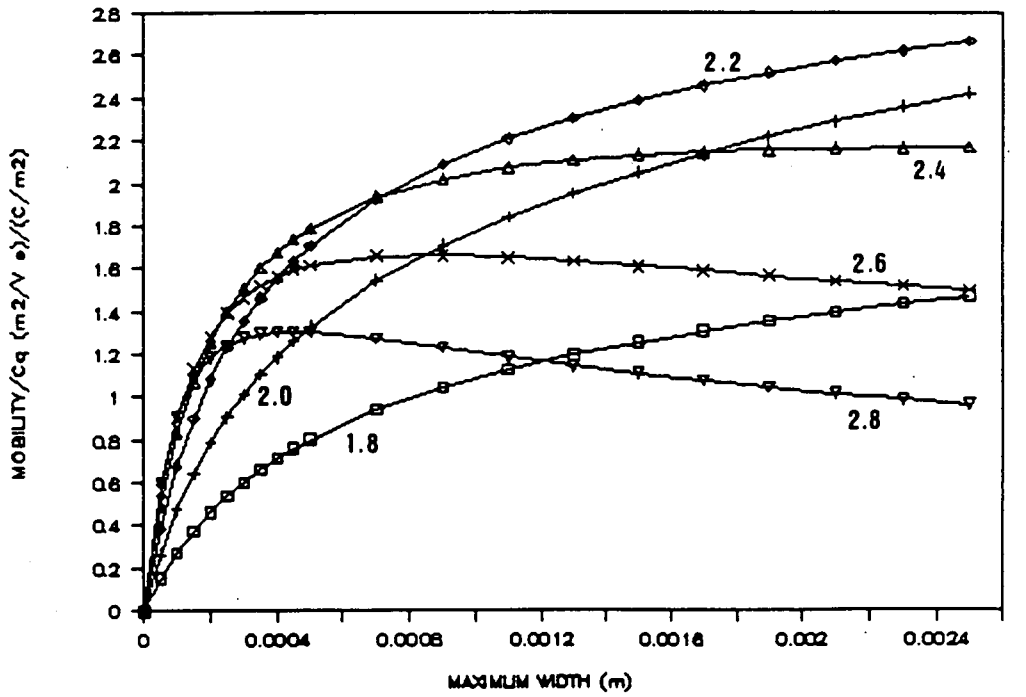

Figure 22. Mobilities of plane form ice crystals at the 400 mb level for values of density exponent N of 1.8, 2, 2.2, 2.4 and 2.8.

altitudes of plane form ice crystals with a density exponent N of 2.2 are shown in Figure 23 and the corresponding normalized mobilities are shown in Figure 24.

3.3 COLUMNAR ICE CRYSTALS

Using the relationships given in Section 2.3 equations can be derived for the velocities and mobilities as functions of the pressure and crystal length as was done for the spherical ice particles.

$$U - U_a = 1 / \Sigma_6 (a_i \, 10^{ji} \, L^{ki} \, p^{li}) \cdot (m/s) \qquad (47)$$

The values for the coefficients in this expression are given in Table 13

TABLE 13

i	a_i	j_i	k_i	l_i
1	6.630	6-5.0 N	(1-N)	0.1522
2	1.299	4-3.125N	0.625(1-N)	0.2790
3	4.616	1-1.25 N	0.25 (1-N)	0.4057
4	6.656	-1-2.5 N	-0.5 -0.5 N	0.1522
5	-2.361	-4-0.625N	-0.875-0.125N	0.2790
6	-7.423	-8+1.25 N	-1.25 +0.25 N	0.4057

$$B = C_q / \Sigma_3 (b_i \, 10^{mi} \, L^{ni} \, p^{oi}) \quad (m^2/V\,s) \qquad (48)$$

The values for the coefficients in this expression are given in Table 14

TABLE 14

i	b_i	m_i	n_i	o_i
1	-3.55+2.38 $N^{0.5}$	-4	-1.0	0.1522
2	7.09-4.13 $N^{0.5}$	-2	-0.5	0.2790
3	3.22+0.111 N^5	0	+0.5	0.4057

Plots of the sedimentation velocities of columnar ice crystals at the 400 mb level for a range of values of N are given in Figure 25

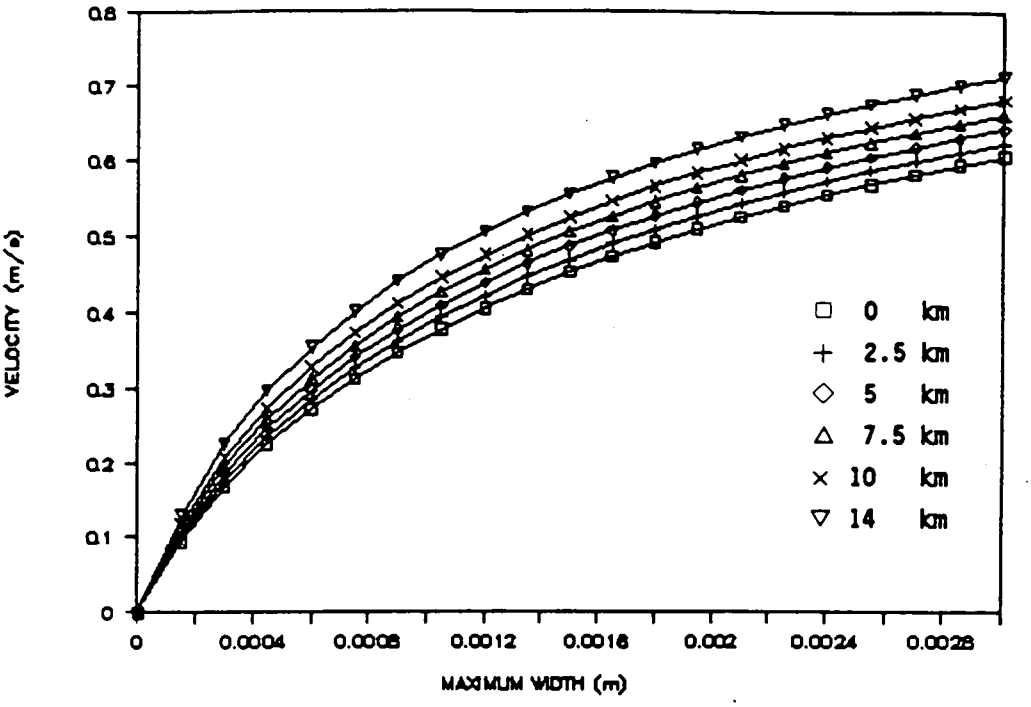

Figure 23. Fall velocities of plane form ice crystals with values of density exponent N of 2.2 at 0, 2.5, 5, 7.5, 10, and 14 km.

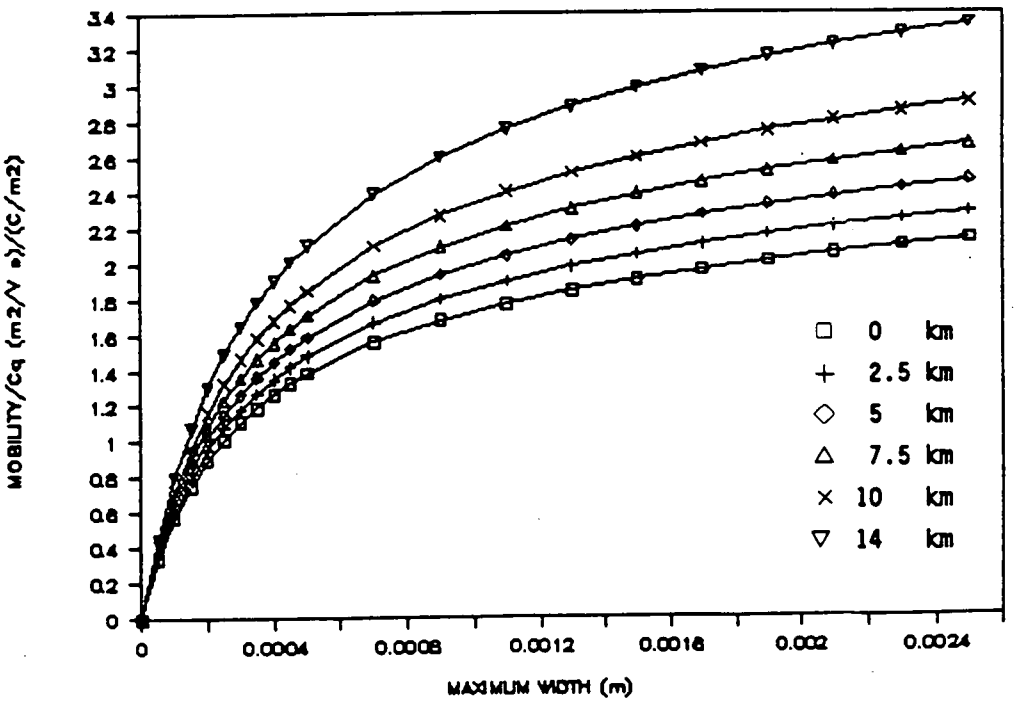

Figure 24. Mobilities of plane form ice crystals with values of density exponent N of 2.2 at 0, 2.5, 5, 7.5, 10, and 14 km.

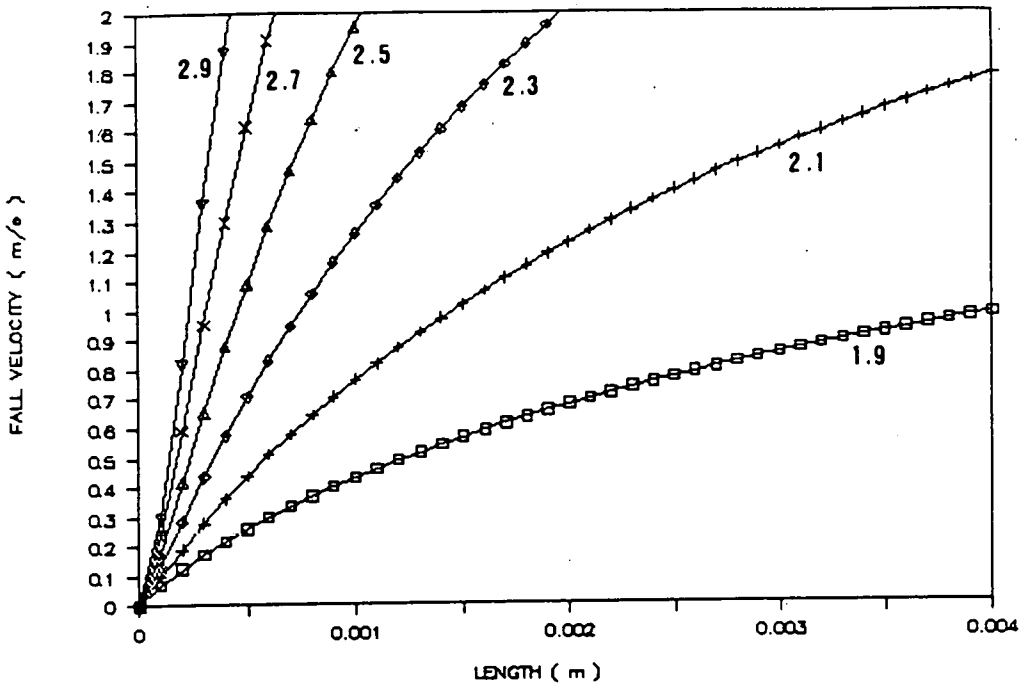

Figure 25. Fall velocities of columnar ice crystals at the 400 mb level for values of density exponent N of 1.9, 2.1, 2.3, 2.5, 2.7, and 2.9.

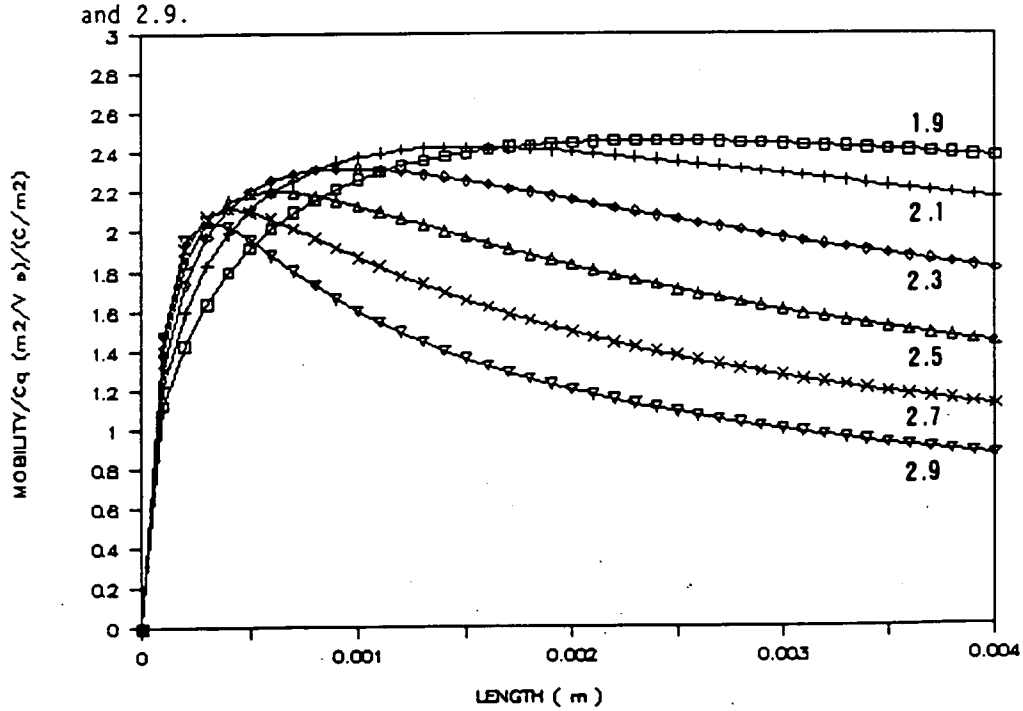

Figure 26. Mobilities of columnar ice crystals at the 400 mb level for values of density exponent N of 1.9, 2.1, 2.3, 2.5, 2.7, and 2.9.

and the corresponding normalized mobilities are shown in Figure 26. Plots of the fall velocities at several different altitudes of columnar ice crystals with a density exponent N of 2.2 are shown in Figure 27 and the corresponding normalized mobilities are shown in Figure 28.

3.4 CONICAL FORM PARTICLES

Using the relationships given in Section 2.4 equations for the velocities and mobilities can be obtained for the conical form particles as functons of the diameter, particle density and atmospheric pressure.

The expression for the velocity obtained from Equation (32) is,

$$U - U_a = 1 / \Sigma_3 \left(a_i \, \Delta\rho^{ji} \, p^{ki} \, d^{li} \right) \text{ (m/s)} \qquad (49)$$

The values for the coefficients in this expression are given in Table 15

TABLE 15

i	ai	ji	ki	li
	A. 90° CONE-SPHERICAL SEGMENT			
1	1.252E-04	-1.00	0.1522	-2.00
2	-5.561E-03	-0.75	0.2790	-1.25
3	5.522E-01	-0.50	0.4507	-0.50
	B. 70° CONE-SPHERICAL SEGMENT			
1	1.658E-04	-1.00	0.1522	-2.00
2	-7.647E-03	-0.75	0.2790	-1.25
3	4.870E-01	-0.50	0.4507	-0.50
	C. 90° CONE-HEMISPHERE			
1	1.021E-04	-1.00	0.1522	-2.00
2	-4.413E-03	-0.75	0.2790	-1.25
3	3.925E-01	-0.50	0.4507	-0.50
	D. 90° TEARDROP			
1	5.051E-05	-1.00	0.1522	-2.00
2	-1.184E-03	-0.75	0.2790	-1.25
3	2.362E-01	-0.50	0.4507	-0.50

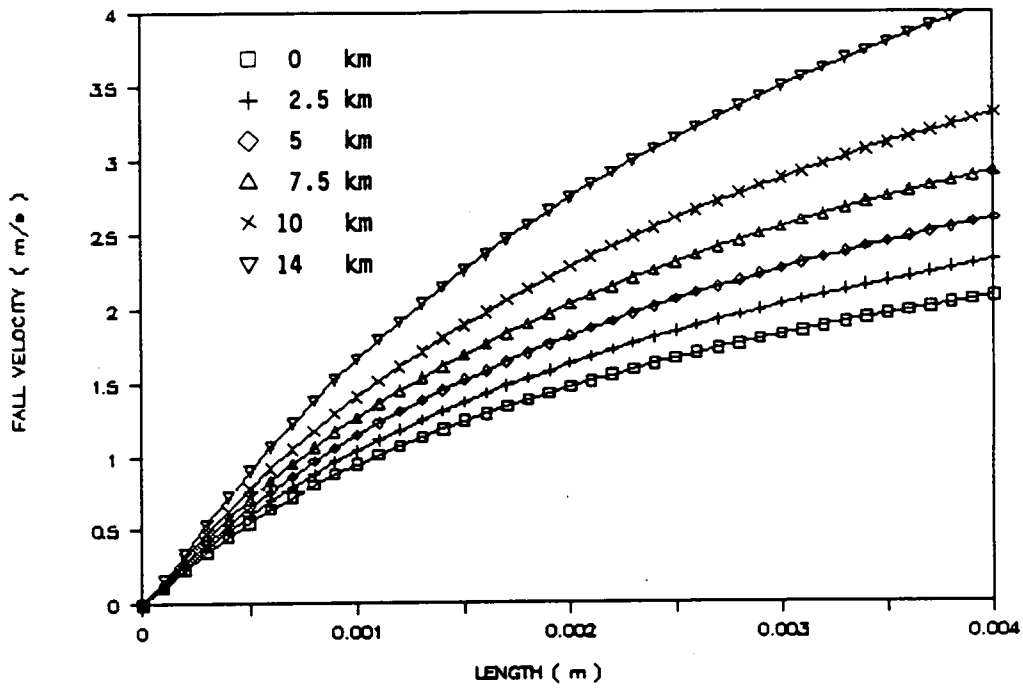

Figure 27. Fall velocities of columnar ice crystals with values of density exponent N of 2.3 at 0, 2.5, 5, 7.5, 10, and 14 km.

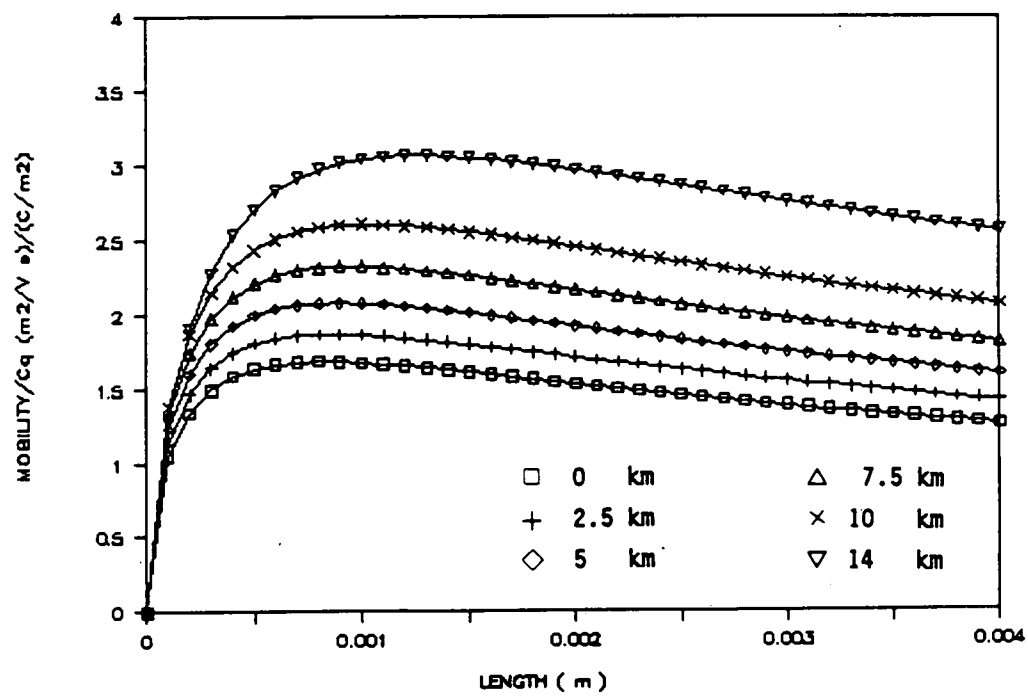

Figure 28. Mobilities of columnar ice crystals particles with values of density exponent N of 2.3 at 0, 2.5, 5, 7.5, 10, and 14 km.

and for the mobility is,

$$B = C_q \; / \; \Sigma_3 \; (\; b_i \; \Delta\rho^{mi} \; p^{ni} \; d^{oi} \;) \; (m^2/V \; s) \qquad (50)$$

The values for the coefficients in this expression are given in Table 16

TABLE 16

i	bi	mi	ni	oi
	A. 90° CONE-SPHERICAL SEGMENT			
1	1.331E-04	0.0252	0.1473	-1.00
2	-1.122E-02	0.2716	0.2544	-0.25
3	1.256E+00	0.4909	0.3980	0.50
	B. 70° CONE-SPHERICAL SEGMENT			
1	1.733E-04	0.0595	0.1702	-1.00
2	-1.353E-02	0.3155	0.2885	-0.25
3	1.286E+00	0.5010	0.4019	0.50
	C. 90° CONE-HEMISPHERE			
1	1.328E-04	0.0365	0.1566	-1.00
2	-1.081E-02	0.2844	0.2682	-0.25
3	1.150E+00	0.4938	0.3990	0.50
	D. 90° TEARDROP			
1	7.417E-05	0.0185	0.1517	-1.00
2	-3.915E-03	0.2836	0.2591	-0.25
3	6.883E-01	0.4955	0.4005	0.50

Plots of the sedimentation velocities of four conical forms of particles at a pressure of 400 mb with a density of 800 kg/m^3 are given in Figure 29 and the corresponding normalized mobilities are shown in Figure 30.

3.5 WATER DROPS AND DROPLETS

Using the relationships given in Section 2.5 equations have been derived for the velocities and mobilities of water drops as a function of the equivalent diameter and the atmospheric pressure. It was found necessary to use a four term series for each parameter

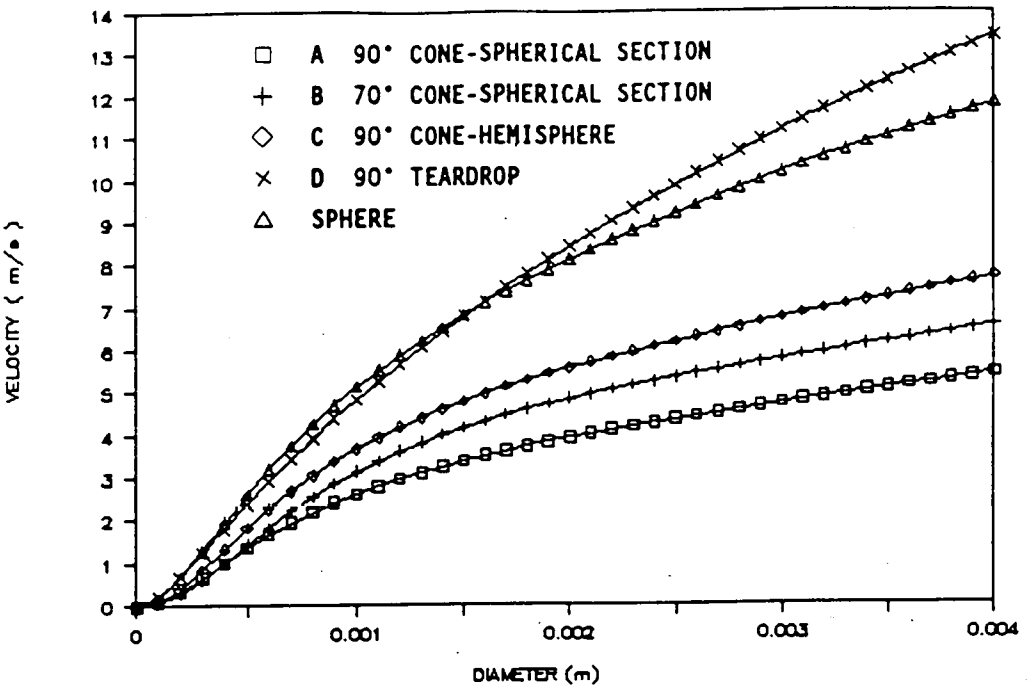

Figure 29. Fall velocities of conical form and spherical particles with a density of 800 kg/m^3 at a pressure of 400 mb.

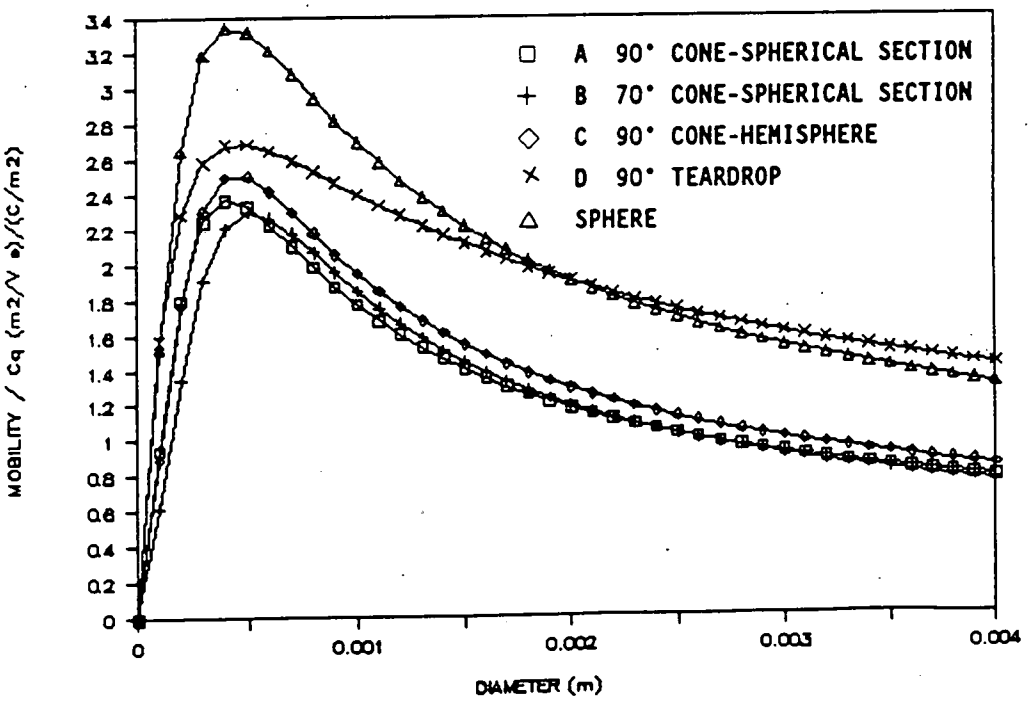

Figure 30. Normalized mobilities of conical form and spherical particles with a density of 800 kg/m^3 at a pressure of 400 mb.

because of the large changes in drag coefficient caused by drop distortion for drops larger than about 0.5 mm.

$$U - U_a = 1 / \Sigma_4 (a_i 10^{ji} L^{ki} p^{li}) \quad (m/s) \qquad (51)$$

The values for the coefficients in this expression are given in Table 17

TABLE 17

i	a_i	j_i	k_i	l_i
1	3.056	-8	-2.00	0.1323
2	8.493	-6	-1.25	0.2699
3	5.462	-3	-0.50	0.4137
4	5.284	0	+1.00	0.4760

$$B = C_q / \Sigma_4 (b_i 10^{mi} d^{ni} p^{oi}) \quad (m^2/V\ s) \qquad (52)$$

The values for the coefficients in this expression are given in Table 18

TABLE 18

i	b_i	m_i	n_i	o_i
1	5.746	-5	-1.0	0.1522
2	7.160	-3	-0.25	0.1604
3	1.806	+1	+0.5	0.4199
4	1.664	+4	+2.0	0.4733

Plots of the sedimentation velocities of water drops are given in Figure 31 and the corresponding normalized mobilities are shown in Figure 32.

4. CONCLUSIONS

Section 2 of this paper gives general equations for the Reynolds number of a variety of types of ice crystals and water drops in terms of the Davies, Bond, and Knudsen numbers. The equations are in terms of the basic physical parameters of the system and are valid for calculating velocities in gravitational and electric fields over

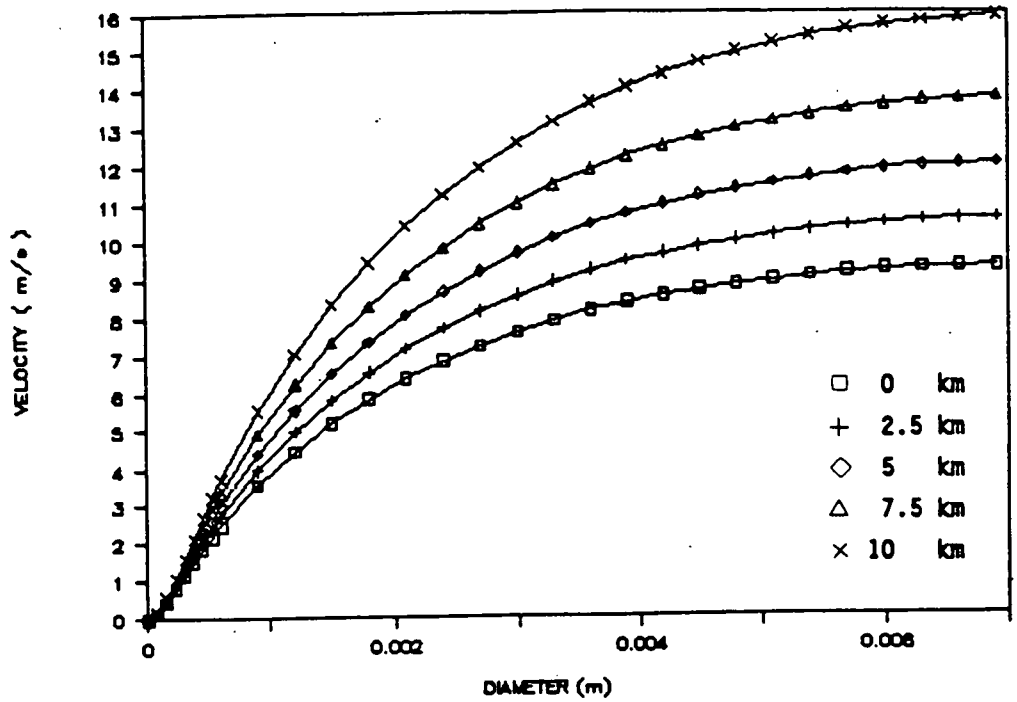

Figure 31. Fall velocities of water drops at 0, 2.5, 5, 7.5, and 10 km.

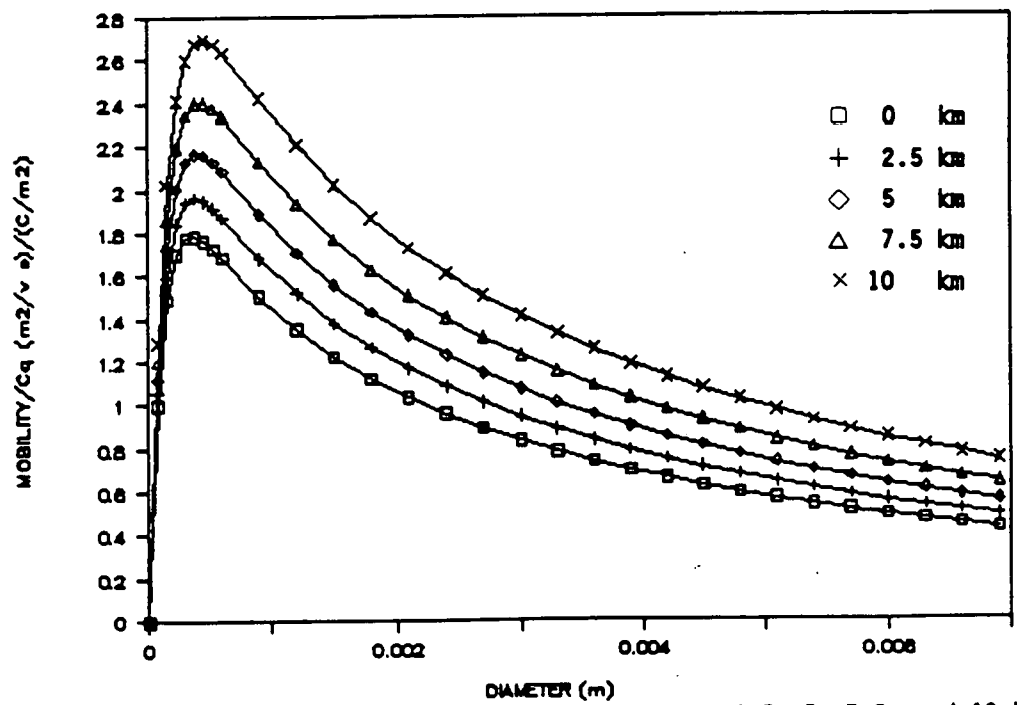

Figure 32. Mobilities of of water drops at 0, 2.5, 5, 7.5, and 10 km.

a very wide range of sizes and atmospheric conditions. The equations are asymptotically matched at the bottom and top of the size spectrum, a useful attribute when checking large computer codes.

A numerical system for specifying the dimensional properties of ice crystals has been introduced as an adjunct to more subjective classification schemes. This allows the observed dimensional statistical properties of an ensemble of particles to be related to the statistical properties dependent on transport.

It is important to realize that particles in the atmosphere come in a broad spectrum of sizes, forms, and densities. Riming and aggregation greatly increase the variability in the transport velocities. When one is dealing with properties of the ensemble such as the mass density, the conductivity, or the energy, for example, it is necessary to integrate over statistical distributions because the variation about a mean value is usually so large. The expressions in this paper have been developed with this in mind.

Within the limits imposed by such variables as particle density, which have large deviations, the accuracy of velocities appear to be within about 10% over the entire range of sizes of interest when compared with such data as are available. Particular attention has been given to ensuring that at the lower end of the size distribution values tend to reasonable limits. Because of the behavior of the drag coefficient as size decreases negative velocities are a common feature of empirical expressions for particle velocities expressed as power series in a length parameter. Such an artifact can have serious consequences in a computer code.

Conical form ice crystals present special problems for the development of simple equations of motion because of the varying aspects they present and the oscillatory motions they exhibit. The relations given here should at least allow reasonable estimates to be made of the range of variability likely to be produced by shape variations

Section 3 gives simple equations in a uniform format for the terminal velocity and normalized mobility for a wide range of sizes and habits of ice srystals, and water drops in terms of the atmospheric pressure and an appropriate size parameter. These equations are simpler to use for many purposes and have comparable accuracies and ranges of application with the more basic formulas given in Section 2.

APPENDIX

LIST OF SYMBOLS.

a/b = the ratio of the major diameter to the height of a water drop.

A_C is the cross sectional area of a crystal in a plane normal to the motion. (m^2)

A_D is the cross sectional area of a circular disc of diameter W,

$A_D = \pi W^2 / 4$ (m^2)

A_S is the total surface area of a crystal (m^2)

B is the mobility of a particle = $\Delta U / E$ ($m\ V^{-1}\ s^{-2}$)

C_d is the drag coefficient.

$C_d = N_D / N_R^2$

C_q is the charge per unit area on a particle (C/m^2)

$C_q = q / A_S$ (C/m^2)

d is the particle diameter (m)

For crystals of columnar form d is the length along the a-axis.

For water drops of ellipsoidal shape with major diameter a and height b the equivalent drop diameter is,

$d = a^{2/3}\ b^{1/3}$ (m)

d_0 is the diameter of a sphere of mass m_0 and density $\Delta\rho_0$.

The value assumed here is, $d_0 = 1\ 10^{-5}$ (m)

D is the drag force, (N)

E is the electric field. (V/m)

F is the force on the particle (N)

g is the gravitational acceleration ($m\ s^{-2}$)

l is the mean free path (m)

Using the effective collision diameter of mean air from the US Standard Atmosphere [1976] gives,

$l = 2.33E\text{-}10\ T / p$ (m)

L is the length of a columnar form crystal along the c-axis. (m)

m is the mass of a particle, (kg)

$m_0 = (\pi \Delta\rho_0 / 6)\ d_0^3$ (kg)

with the values adopted here for $\Delta\rho_0$ and d_0

$m_0 = 5.236\ 10^{-13}$ (kg)

N is the exponent of the density

for particles of plane form $N = \log(m\ d_0)/\log(m_0\ W)$

for particles of columnar form $N = \log(m\ d_0)/\log(m_0\ L)$

N_{Bo} the Bond number is a nondimensional parameter relating the pressure on the surface to the surface tension,

$N_{Bo} = 6\ F / (\pi\ d\ \sigma)$

N_D is the Davies or Best number, a nondimensional parameter related to the force on the particle, $N_D = (8 \rho / \pi \eta^2) F$

N_K is the Knudsen number, the ratio of the mean free path to the particle diameter, $N_K = l / d$

N_R is the Reynolds number $N_R = (\rho d / \eta) (U - U_a)$

p is the atmospheric pressure (bar)

1 $N/m^2 = 10^{-5}$ bar

q is the charge on the particle, (C)

t is the time, (s)

T is the air temperature (K)

U is the particle velocity (m/s)

U_a is the air velocity (m/s)

W is the maximum width of a plane form crystal (m)

X is the modified Davies number for a column $X = (2 \rho d /(L \eta^2)) F$

η is the dynamic viscosity of air (kg/m s)

ρ is the air density (kg m^{-3})

$\Delta\rho$ is the difference between the particle and air density (kg/m^3)

σ is the surface tension of water against air (N/m)

$\sigma = 0.1165-1.492\ 10^{-4}\ T$ for $265\ K < T < 303\ K$ (N/m)

ACKNOWLEDGMENTS.

The research reported in this paper was supported by the National Aeronautics and Space Administration under Grant Number NGL 39-009-003

REFERENCES

Abraham, F. F., Functional dependence of drag coefficient of a sphere on Reynolds number, *Phys. Fluids*, **13**, 2194-2195, 1970.

Auer, A. H., Observations of ice crystal nucleation by droplet freezing in natural clouds, *J. Atmos. Sci.*, **28**, 285-290, 1971.

Auer, A. H., Distribution of graupel and hail with size, *Monthly Weather Review*, **100**, 325-328, 1972a.

Auer, A. H., Inferences about ice nucleation from ice crystal observations, *J. Atmos. Sci.*, **29**, 311-317, 1972b.

Auer, A. H., and D. L. Veal, The dimensions of ice crystals in natural clouds, *J. Atmos. Sci.*, **27**, 919-926, 1970.

Bashkirova, G. M., and T. A. Pershina, On the mass of snow crystals and their fall velocity, *Tr. Gl. Geophiz. Observ.*, **156**, 83-100, 1964.

Beard, K. V., Terminal velocity and shape of cloud and precipitation drops aloft, *J. Atmos. Sci.*, **33**, 851-864, 1976.

Beard, K. V., and H. R. Pruppacher, A determination of the terminal velocity and drag of small water drops by means of a wind tunnel, *J. Atmos. Sci.*, **26**, 1066-1072, 1969.

Berry, E. X., and M. R. Pranger, Equations for calculating the terminal velocities of water drops., *J. Appl. Meteor.*, **13**, 108-113, [1974],

Best, A. C., Empirical formulae for the terminal velocity of water drops falling through the atmosphere, *Quart. J. Roy. Meteor. Soc.*, **76**, 302-311, 1950.

Bilham, E. G., and E. F. Relf, The dynamics of large hailstones, *Quart. J. Roy. Meteor. Soc.*, **63**, 149-162, 1937.

Blanchard, D. C., The behavior of water drops at terminal velocity in air, *Trans. Amer. Geophys. Union*, **31**, 836-842, 1950.

Blanchard, D. C., Comments on "On the shape of water drops falling in stagnant air", *J. Meteor.*, **12**, 91-92, 1955.

Davies, C. N., Definitive equations for the fluid resistance of spheres, *Proc. Roy. Phys. Soc. London*, **A57**, 259-270, 1945.

Epstein, P. S. On the resistance experienced by spheres in their motion through gas. *Phys. Rev.*, **23**, 710-733, 1924.

Fitzgerald, D., and H. R. Byers, *Res. Rept., AF 19(604)2189*, Dept. Meteorology, University of Chicago, Chicago, Ill., 1962.

Flower, W. D., The terminal velocity of drops, *Proc. Roy. Phys. Soc. London*, **A40**, 167-176, 1928.

Green, A. W., An approximation for the shapes of large raindrops, *J. Appl. Meteor.*, **14**, 1578-1583, 1975.
Gunn, R., The free electrical charge on thunderstorm rain and its relation to droplet size, *J. Geophys. Res.*, **54**, 57-63, 1949.
Gunn, R and G. D. Kinzer, The terminal velocity of fall for water droplets in stagnant air , *J. Meteor.*, **6**, 243-248, 1949
Herzegh, P. H. and P. V. Hobbs, Size spectra of ice particles in frontal clouds: correlations between spectrum shape and cloud conditions, *Quart. J. R. Met. Soc.*, **111**, 463-477, 1985.
Heymsfield, A., Ice crystal terminal velocities, *J. Atmos. Sci.*, **29**, 1348-1357, 1972.
Hobbs, P. V., S. Chang and J. D. Locatelli, The dimensions and aggregation of ice crystals in natural clouds, *J. Geophys. Res.*, **79**, 2199-2206, 1974.
Holitza, F. J., and H. W. Kasemir, Accelerated decay of thunderstorm electric fields by chaff seeding, *J. Geophys. Res.*, **79**, 425-429, 1974.
Jayaweera, K. O. L. F., An equivalent disc for calculating the terminal velocities of plate-like ice crystals, *J. Atmos. Sci.*, **29**, 596-598, 1972.
Jayaweera, K. O. L. F., and R. E. Cottis, Fall velocities of plate-like and columnar ice crystals, *Quart. J. R. Met. Soc.*, **95**, 703-709, 1969.
Jayaweera, K. O. L. F., and B. J. Mason, The behaviour of freely falling cylinders and cones in a viscous fluid, *J. Fluid Mech.*, **22**, 709-720, 1965.
Jayaweera, K. O. L. F., and B. J. Mason, The falling motion of loaded cylinders and disks simulating snow crystals, *Quart. J. R. Met. Soc.*, **92**, 151-156, 1966.
Jones, D. M., The shape of raindrops, *J. Meteor.*, **16**, 504-510, 1959.
Kajikawa, M., A model experimental study on the falling velocity of ice crystals, *J. Meteor. Soc. Japan*, **49**, 367-375, 1971
Kajikawa, M., Measurement of falling velocity of individual snow crystals, *J. Meteor. Soc. Japan*, **50**, 577-583, 1972
Knudsen, M., and S. Weber, Resistance to motion of small spheres. *Ann. Phys.*, **36**, 981-994, 1911.
Kumai, M., Microspherules in snow and ice crystals, *J. Geophys. Res.*, **71**, 3397-3404, 1966.

Kumai, K., and K. Itagaki, Shape and fall velocity of natural raindrops, *J. Meteor. Soc. Japan*, **32**, 11-18, 1954.
Laws, J. O., Measurements of the fall velocity of water drops and rain drops, *Trans. Am. Geophys. Union*, **22**, 709-721, 1941.
LeClair, B. A., A. E. Hamielec and H. R. Pruppacher, A numerical study of the drag on a sphere at low and intermediate Reynolds numbers, *J. Atmos. Sci.*, **27**, 308-315, 1970.
Lenard, P., Uber regen, *Meteor. Zeit.*, **21**, 249-262, 1904.
List R., Zur Aerodynamik von Hagelkörnern, *Z. Angew.Math. Phys.*, **10**, 143-159, 1959
List R., On the simulation of physical processes ocurring in clouds, *Bull. Amer. Meteor. Soc.*, **47**, 393-396, 1966.
List, R., and R. S. Schemenauer, Free-fall behavior of planar snow crystals, conical graupel and small hail, *J. Atmos. Sci.*, **28**, 110-115, 1971.
Liu, C. M., Effects of the raindrop terminal velocity on raindrop growth, *Papers in Meteor. Res., Taipei*, **9**, 79-103, [1986]
Liu, J. Y.,and H. D. Orville, Numerical modeling of precipitation and cloud shadow effects on mountain-induced cumuli, *J. Atmos. Sci.*, **26**, 1283-1298, [1969],
Locatelli, J. D., and P. V. Hobbs, Fall speeds and masses of solid precipitation particles, *J. Geophys. Res.*, **79**, 2185-2197, 1974.
Macklin, W. C., and F. H. Ludlam, The fallspeeds of hailstones , *Quart. J. Roy. Meteor. Soc.*, **87**, 72-81, 1961.
Magono, C., and C. W. Lee, Meteorological classification of natural snow crystals, *J. Fac. Sci. Hokkaido Univ., Ser 7*, **2**, 321-335, 1966.
Magono, C., On the shape of water drops falling in stagnant air, *J. Meteor.*, **11**, 77-79, 1954.
Manton, M. J., and W. R. Cotton, Formulation of approximate equations for modeling moist deep convection on the mesoscale, *Atmos. Sci. Paper No 266*, Dept. of Atmos. Sci., Colo. State Univ., Ft. Collins.
Nakaya, U., and T. Terada, Simultaneous observations of the mass, falling velocity and form of individual snow crystals, *J. Fac. Sci. Hokkaido Imp. Univ., Ser 2*, **1**, 191-200, 1935.
Ogura Y., and T. Takahashi, The development of warm rain in cumulus model, *J. Atmos. Sci.*, **30**, 262-277, [1973],
Ono, A., The shape and riming properties of ice crystals in natural clouds, *J. Atmos. Sci.*, **26**, 138-147, [1969],

Perry, J., *Chemical Engineering Handbook*. 3rd ed. McGraw-Hill, 1017 pp., 1950.
Podzimek J., Aerodynamic conditions for ice crystal aggregation, *Proc. Cloud Phys. Conf., Toronto*, 295-299, University of Toronto Press, Toronto, 1968.
Pruppacher, H. R., and K. V. Beard, A wind tunnel investigation of the internal circulation and shape of water drops falling at terminal velocity in air, *Quart. J. R. Meteor. Soc.*, **96**, 247-256, 1970.
Pruppacher, H. R., and J. D. Klett, *Microphysics of clouds and precipitation*, D. Reidel Publishing Co., Dordrecht, 1978.
Pruppacher, H. R., and R. Pitter, A semi-empirical determination of the shape of cloud and rain drops, *J. Atmos. Sci.*, **28**, 86-94, 1971.
Roos, D. S., A giant hailstone from Kansas in free fall, *J. Appl. Meteor.*, **11**, 1008-1011, 1972.
Shiino, J.I., Evolution of raindrops in an axisymmetric cumulus model. Part I. Comparison of the parameterized with non-parameterized microphysics, *J. Meteor. Soc. Japan*, **61**, 629-655, [1983],
Takahashi, T., Measurement of electric charge on cloud droplets, drizzle, and raindrops, *Rev. Geophys. Space Phys.*, **11**, 903-924, 1973.
US Standard Atmosphere, 1966, U. S. Government Printing Office, Washington, D. C., 1966.
US Standard Atmosphere, 1976, U. S. Government Printing Office, Washington, D. C., 1976.
Winn, W. P., G. W. Schwede, and C. B. Moore, Measurement of electric fields in thunderclouds, *J.Geophys. Res.*, **79**, 1761-1767, 1974.
Yagi, T., Measurement of the fall velocity of ice crystals drifting in supercooled fog, *J. Meteor. Soc. Japan*, **48**, 287-292, 1970.
Zikmunda, J., and G. Vali, Fall patterns and Fall velocities of rimed ice crystals, *J. Atmos. Sci.*, **29**, 1334-1347, 1972.